Supplementary Information (SI) for Inorganic Chemistry Frontiers.

Supplementary Information

Electron transport chain-inspired photodiode-like junction in metal-organic framework for directional multi-electron transfer in photocatalysis

Yang An,[a] Muhammad Saqaf Jagirani,[a] Xu Zhang,[a] Lanqiao Li,[a] Yu Zou,[a] Lei Qiao,[a] Renhai Liu,[a] Abdoulkader Ibro Douka,[a] Rui Cai,[a] Cheng He,[a] Tiexin Zhang,*[a] Yusheng Shi*[b] and Chunying Duan*[c]

[a] State Key Laboratory of Fine Chemicals, School of Chemistry, Frontier Science Center for Smart Materials, School of Chemical Engineering, Dalian University of Technology, Dalian 116024, China. E-mail: zhangtiexin@dlut.edu.cn

[b] State Key Laboratory of Structural Chemistry, Fujian Institute of Research on the Structure of Matter, Chinese Academy of Sciences, Fuzhou 350002, P. R. China. E-mail: shiyusheng@fjirsm.ac.cn

[c] State Key Laboratory of Coordination Chemistry, Nanjing University, Nanjing 210023, P. R. China. E-mail: cyduan@dlut.edu.cn

Table of Contents

1. Materials and Methods

All reactants used were purchased commercially and used without further purification; the **PTH** carboxylic ligand was synthesised according to the reported method.[1]

Scanning electron microscopy (SEM) images were captured using a SU8220. N_2 adsorption-desorption isotherms were measured using an Autosorb iQ at 77 K. ^1H and ^{13}C NMR spectra were recorded on Bruker 400 MHz, 500 MHz, or 600 MHz spectrometers, and chemical shifts were reported in parts per million (ppm, δ) relative to tetramethylsilane as the internal standard. Electron paramagnetic resonance (EPR) spectra were acquired on Bruker A200-9.5/12 in N_2 atmosphere. The powder X-ray diffraction (PXRD) diffractograms were obtained on a Rigaku D/Max-2400 X-ray diffractometer with a sealed Cu tube (λ = 1.54056 Å). Liquid UV-vis spectra were recorded on a TU-1900 spectrophotometer. Solid UV-vis spectra were recorded on a Hitachi U-4100 UV-vis-NIR spectrophotometer. Fluorescent spectra and photoluminescence decay profiles were recorded on an Edinburgh FLS 1000 stable/transient fluorescence spectrometer. FT-IR spectra were recorded using KBr as pellets on a NEXUS instrument. X-ray photoelectron spectroscopy (XPS) signals were collected on a Thermo ESCALAB Xi^+ spectrometer.

Electrochemical impedance spectroscopy (EIS) and photocurrent measurements were performed in a standard three-electrode system, with the photocatalyst-coated fluorine-doped tin oxide (FTO) serving as the working electrode. The measurements were recorded on a CHI 760E electrochemical workstation. A Pt plate was used as the counter electrode, and Ag/AgCl was used as the reference electrode. A 365 nm LED was used as the light source. A 0.1 M DMF solution of ammonium hexafluorophosphate was used as the electrolyte. 2 mg of the metal-organic framework was added to a mixed solution containing 20.0 μL of 5 wt% Nafon and 1 mL of ethanol. The working electrodes were prepared by dropping 100 µL of the suspension onto the surface of an FTO plate with an area of 1.0 cm^2.

CV was record on ZAHNER ENNIUM Electrochemical Workstation with a typical three electrodes system, for the metal-organic framework (MOF), MOF-coated FTO served as working electrode, Ag/AgCl as the reference electrode, a Pt plate was used as the counter electrode, an DMF solution of ammonium hexafluorophosphate (0.1 M) served as the electrolyte. For the ligand, a glassy carbon electrode was used as the working electrode, a Pt plate as the counter electrode, a DMF solution of ammonium hexafluorophosphate (0.1 M) served as the electrolyte, 3 µmol of ligand was added to 3 mL of electrolyte, and the reference electrode was the same as the MOF.

The fs-TA measurements were performed using a Helios Fire spectrometer (Ultrafast Systems LLC) with pump and probe beams derived from an amplified Ti: sapphire laser system (Coherent Astrella, 800 nm, 5.5 mJ $pulse^{-1}$, 35 fs, and 1 kHz repetition rate) at room temperature. A custom-designed fibre-coupled alignment-free spectrometer with a 1024-pixel CMOS sensor (spectral response: 200-1000 nm) was used as the vis/UV-vis detector. Spectral acquisition rate up to 2400 $spectra\cdot s^{-1}$. ADC resolution was 16-bit.

Preparation of the sample: A 5 mg sample was finely ground and dispersed in dimethylformamide (DMF). The resulting suspension was sealed into a quartz cuvette and exchanged with air by bubbling with N_2. Fs-TA data were collected using a previously described home-built setup. Samples were prepared and sealed in a quartz cuvette with a path length of 0.2 cm. Samples were prepared and excited at the specified wavelength such that the percent of molecules excited per pulse was kept near or under 5%. Fs-TA data were fit to an exponential model using an in-house global fitting procedure.

Electron paramagnetic resonance (EPR) measurements were performed using a Bruker E500 spectrometer. To verify the photoinduced electron transfer process, we have tested the spectra of **PTH**@PCN−222(Fe) under irradiation and in the absence of light in a N_2 atmosphere, respectively. *p*-Nitroacetophenone was added to check the reactivity of the intermediate generated after irradiation. The reactive oxygen species (ROS) generated under irradiation were detected in the presence of DMPO in the O_2 atmosphere. 365nm LED was used as the light source.

2. Synthesis and Characterization of PTH@PCN−222(Fe)

Synthesis of PTH ligand

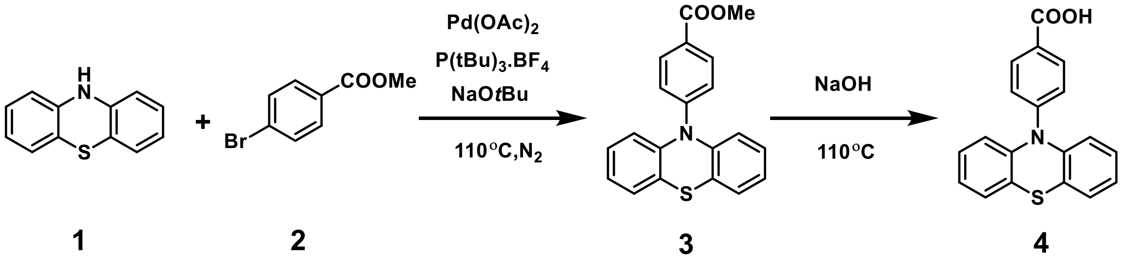

3.0 g of phenothiazine **1** (15 mmol), 3.5 g of methyl 4-bromobenzoate **2** (16 mmol), 180 mg of palladium acetate (0.8 mmol), 1.7 g of sodium *tert*-butoxide (18 mmol), and 0.5 g of tri-*tert*-butylphosphonium tetrafluoroborate (1.7 mmol) were added into a 250 mL three-neck flask, and then subjected to three vacuum/N_2 cycles. Then 80 mL of degassed toluene was added, and the resulting mixture was stirred at 110 °C for 12 hours before it was cooled to room temperature. Toluene was removed under vacuum, and the residual was dissolved in DCM and washed with water. After drying the organic layer with Na_2SO_4, the solvent was evaporated. The pure compound **3** could be obtained by flash chromatography using a DCM: MeOH (v/v) ratio of 100:1 as the eluent, with a yield of 80% (4.0 g). Then, 0.79 g of **3**, 50 mL of THF, 50 mL of MeOH, and 30 mL of aq. solution of NaOH (1M) were added into a three-neck flask, and the reaction mixture was stirred at 100 °C for 12 hrs. After the reaction completed, the solvent was removed by a rotary vacuum evaporator, the residual was re-dissolved in 200 mL water, pH was adjusted to *ca*. 4 by the dropwise addition of dilute HCl, and the precipitated white solid was filtered and washed with acetone and dried in vacuum to obtain 10-(4-carboxyphenyl) phenothiazine **4** (**PTH** carboxylic ligand) in a yield of 70%. ^{1}H NMR (400 MHz, DMSO-d_6) δ 7.99 (d, J = 8.5 Hz, 2H), 7.34 (d, J = 7.5 Hz, 2H), 7.25 (d, J = 8.5 Hz, 2H), 7.20 (t, J = 7.3 Hz, 2H), 7.10 (t, J = 7.3 Hz, 2H), 6.86 (d, J = 7.9 Hz, 2H); ^{13}C NMR (101 MHz, DMSO-d_6) δ 166.90 (s), 146.81 (s), 142.01 (s), 131.66 (s), 127.92 (s), 127.71 (s), 126.79 (s), 126.57 (s), 124.91 (s), 122.42 (s), 121.82 (s). The NMR data matched those previously reported in the literature.[1]

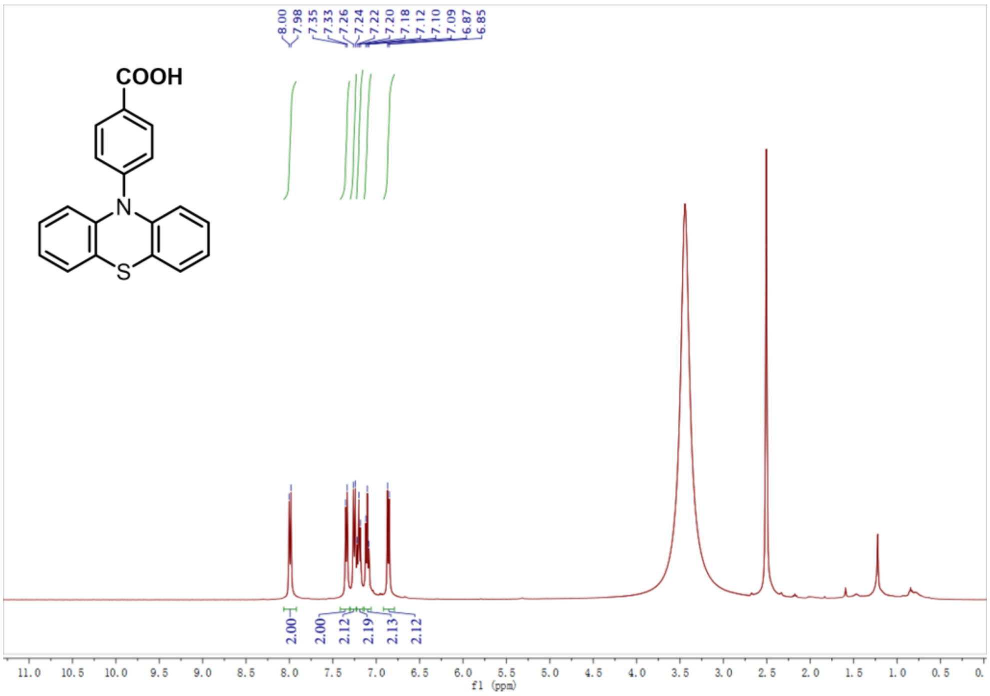

Fig. S1 ^{1}H NMR spectrum of the **PTH** carboxylic ligand.

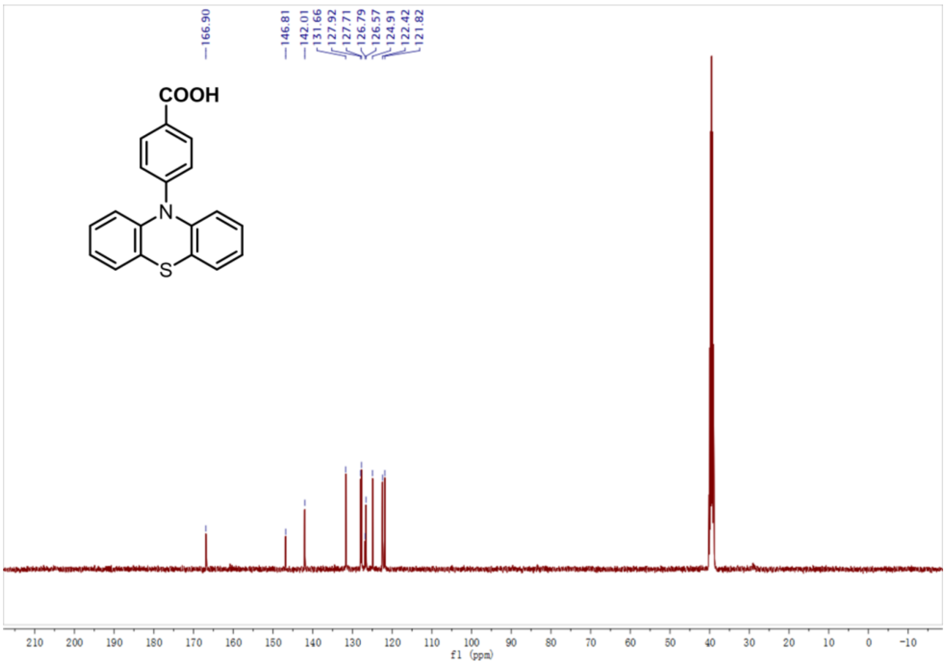

Fig. S2 ^{13}C NMR spectrum of **PTH** carboxylic ligand.

Synthesis and Activation of PCN−222(Fe)

PCN−222(Fe) was synthesised according to the reported protocol.[2] 15 mg $ZrCl_4$ (0.064 mmol), 25 mg Fe−**TCPPCl** (0.030 mmol), and 1.35 g benzoic acid (11.0 mmol) were ultrasonically dissolved in 8 mL of DMF in a 20 mL glass vial. The mixture was heated in a 120 ºC oven for 48 hrs. After cooling to room temperature, the dark brown, needle-like crystals of PCN−222(Fe) were harvested by filtration.

The template reagent, benzoic acid, connected to the Zr6O8 node of PCN−222(Fe) should be removed before loading the PTH carboxylic ligand through the solvent-assisted ligand incorporation (SALI) process. The crystals of PCN−222(Fe) were then activated according to the previously reported protocol for Zr MOFs.[2,3] 200 mg PCN−222(Fe), 100 mL DMF, and 4 mL aqueous solution of HCl (8.0 M) were mixed into a vial, and then heated at 100 ℃ in an oven for 12 hrs. After cooling to room temperature, the solid sample was separated by centrifugation and successively washed with deionised water, acetone, and diethyl ether. It was then dried at 50 °C under vacuum. The activated PCN−222(Fe) was stored in an inert atmosphere in a glove box prior to the SALI process.

Synthesis of PTH@PCN−222(Fe)

260 mg (0.81 mmol) of **PTH** carboxylic ligand, 200 mg (0.156 mmol) of activated PCN−222(Fe),[2,3] and 10 mL of DMF were added into a 50 mL glass vial. The reaction mixture was kept at 100 ºC overnight before being cooled to room temperature. The solid was separated through centrifugation, washed with DMF to remove the unreacted **PTH** ligand from the pores, and then successively washed with acetone and diethyl ether to remove the DMF. It was finally dried under vacuum at 50°C for 3 hrs. The obtained dark brown, needle-like crystals of **PTH**@PCN−222(Fe) were stored in a light-resistant vial and kept in a glove box prior to use.

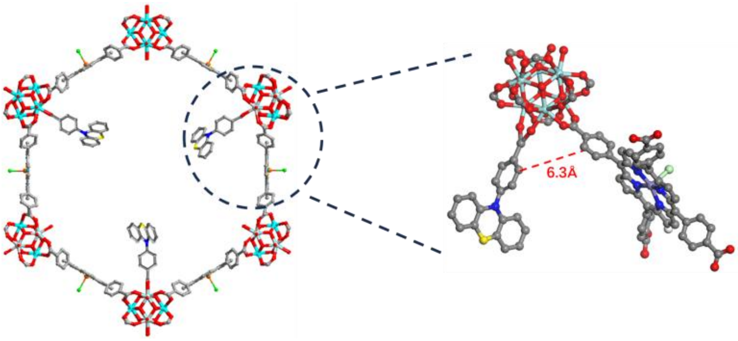

Fig. S3 Schematic diagram of the anchored **PTH** moiety in the pore of **PTH**@PCN−222(Fe).

General Procedure for NMR Characterization of PTH@PCN−222(Fe)

12 mg **PTH**@PCN−222(Fe), 50 µL HF, and 0.5 mL DMSO-*d*$_6$ were added to a plastic vial, and the mixture was sonicated to obtain a clean solution. ^{1}H NMR spectrum of the digested **PTH**@PCN−222(Fe) showed signals corresponding to the **PTH** ligand (2.6 µL of 1,2-dichloroethane as the internal standard); however, it was difficult to determine the precise amount of incorporated phenothiazine moiety owing to the disturbance from the paramagnetic iron porphyrin ligand. Thus, the ratio of the **PTH** carboxylic ligand to the iron porphyrin moiety was roughly estimated to be in the range of 1.7:1.0 to 1.1:1.0.

UV-vis Titration Experiment

By employing the same digestion method for NMR instead of using the undeuterated DMSO, the clear solution of digested **PTH**@PCN−222(Fe) was prepared for further determining the ratio of **PTH** carboxylic ligand vs. iron porphyrin moiety by the UV-vis titration experiment.

Since **PTH**@PCN−222(Fe) was digested by HF, we prepared a reference solution (1 µM) of Fe−**TCPPCl** in DMSO with the same concentration of HF as the digested sample of **PTH**@PCN−222(Fe). Through adding different amounts of PTH ligand into this reference solution, the characteristic n → π* peak at 310 nm of PTH carboxylic ligand and the Soret band of iron porphyrin at 410 nm were chosen to calculate the relative amount of the two ligands through the standard curve. We finally determined the ratio of the PTH carboxylic ligand vs. the iron porphyrin moiety to be 1.5:1.0 (Fig. S4), which is close to the ratio of 1.45:1.0 obtained through EDS elemental analyses (Table S1). These results indicated that each Zr_6O_8 SBU connected three **PTH** carboxylic ligands, and the corresponding molecular weight of **PTH**@PCN−222(Fe) was calculated to be *ca*. 1712.31.

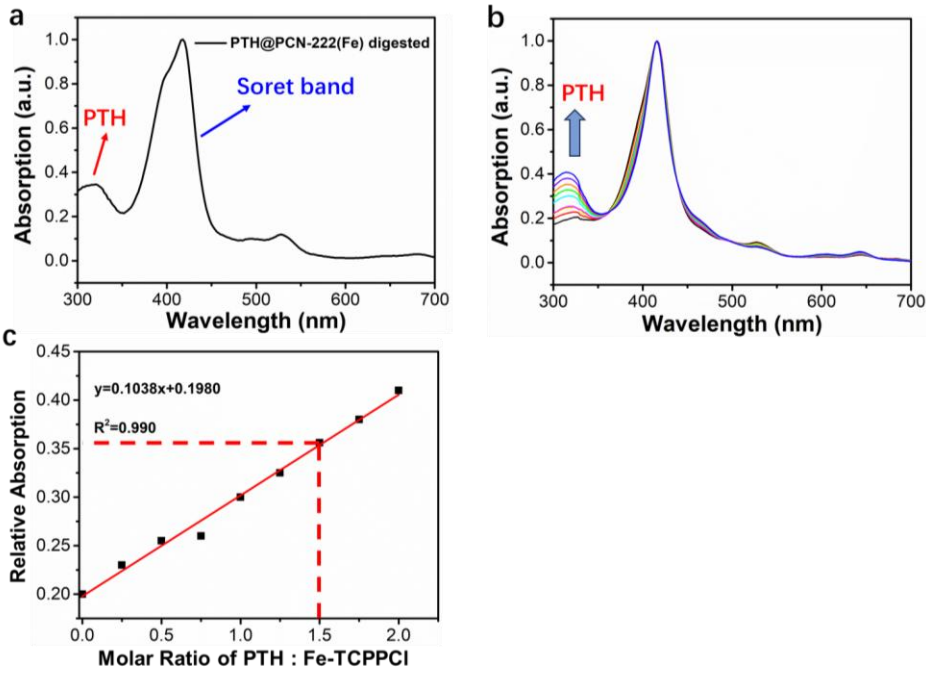

Fig. S4 UV-vis absorption titration experiment. (a) UV-vis spectrum of digested **PTH**@PCN−222(Fe). (b) UV-vis absorption spectra of Fe−**TCPPCl** upon the addition of different amounts of **PTH** ligand. (c) The standard linear relationship between the relative absorption of **PTH** carboxylic ligands/Fe−**TCPPCl** and the relative molar ratio of **PTH** carboxylic ligands/Fe−**TCPPCl**.

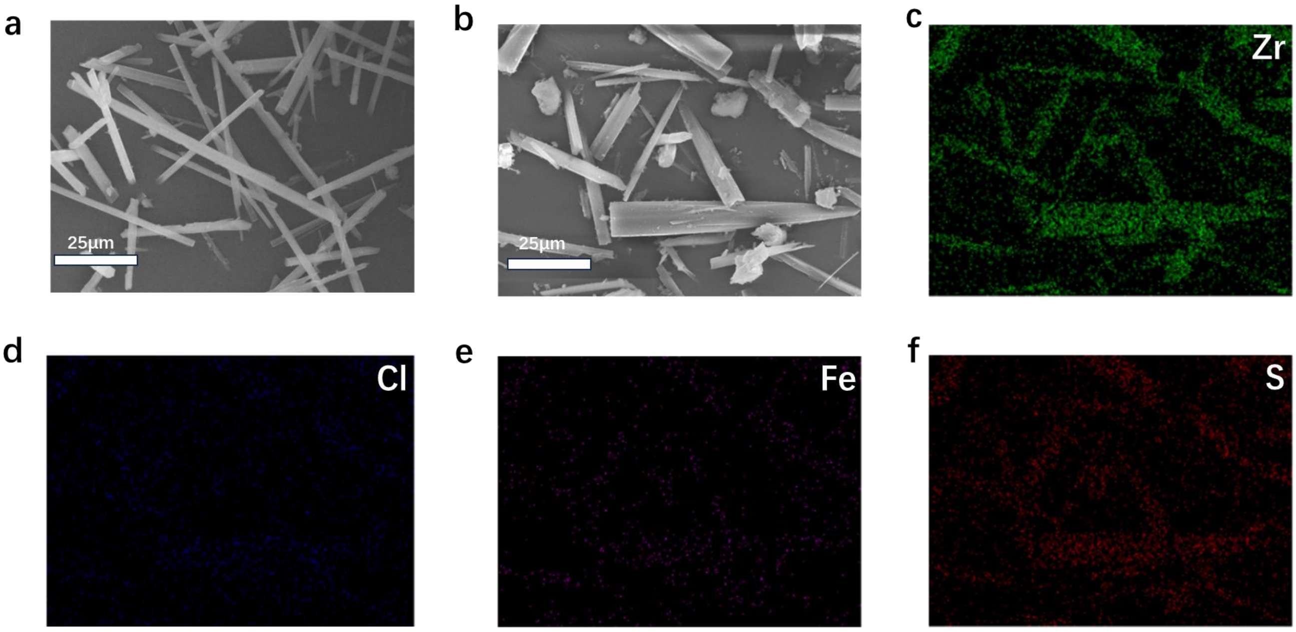

Fig. S5 SEM spectra of (a) PCN−222(Fe) and (b) **PTH**@PCN−222(Fe). Annular dark-field EDS element mapping of **PTH**@PCN−222(Fe) with (c) Zr (green), (d) Cl (blue), (e) Fe (purple), (f) S (red).

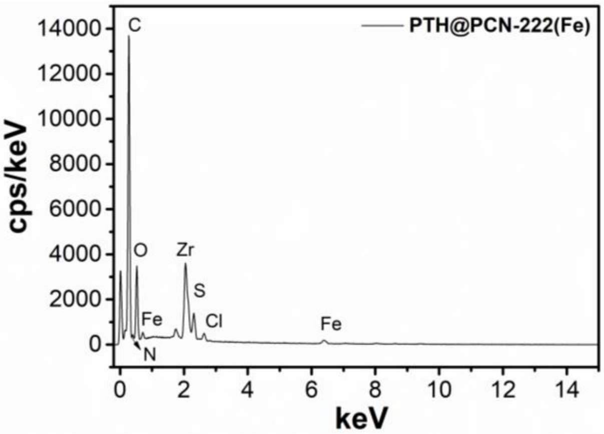

Fig. **S6** SEM-EDS graph of **PTH**@PCN−222(Fe).

Table S1. Elemental analysis results of Zr vs. S in **PTH**@PCN−222(Fe) using SEM-EDS.

Element	Wt%	Atomic %
S	1.94	0.88
Zr	11.43	1.82

3. Investigation on Photoelectronic Properties of PTH@PCN−222(Fe)

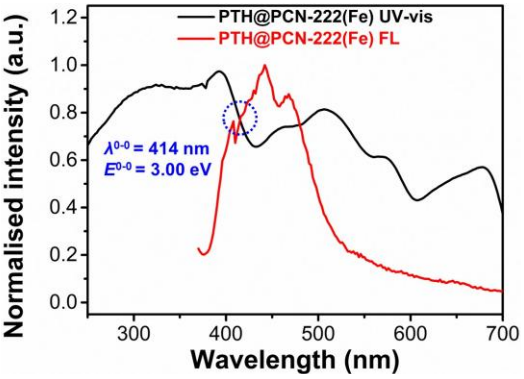

Fig. S7 Normalised UV−vis (black) and fluorescence emission of **PTH**@PCN−222(Fe).

Table S2. The ground-state oxidation potentials, the free energy changes, and the excited-state potentials of **PTH** carboxylic Ligand and MOF **PTH**@PCN−222(Fe), respectively.

	$\boldsymbol{E}(M^+/M)$	$E^{0\text{-}0}$	$E^*(M^+/M^*)$
PTH carboxylic Ligand	1.18 V	3.16 eV	-1.98 V
PTH@PCN−222(Fe)	1.17 V	3.00 eV	-1.83 V

$E^*(cat^{\bullet+}/cat^*) = E(cat^{\bullet+}/cat) – E^{0\text{-}0}$

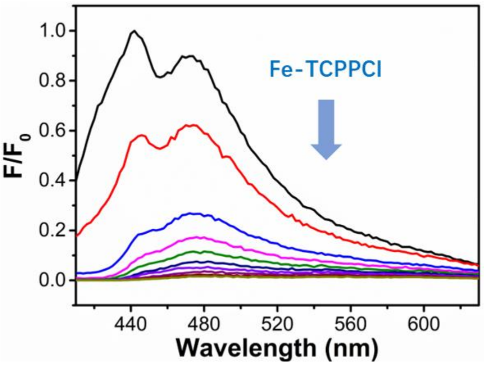

Fig. S8 Photoluminescence spectra of **PTH** carboxylic ligand in DMF upon addition of different amounts of Fe−**TCPPCl**.

Table S3. Photoluminescence lifetime of **PTH** at 440 nm upon the addition of different amounts of Fe−**TCPPCl**.

Entry	Ratio of **PTH** ligand/Fe−**TCPPCl**	Lifetime
PTH ligand		5.9 ns
PTH ligand + 0.2 equiv. Fe−**TCPPCl**	5.0: 1.0	5.8 ns
PTH ligand + 0.4 equiv. Fe−**TCPPCl**	2.5: 1.0	5.5 ns
PTH ligand +0.5 equiv. Fe−**TCPPCl**	2.0: 1.0	5 ns
PTH ligand + 0.67 equiv. Fe−**TCPPCl**	1.5: 1.0	4.6 ns
PTH ligand + 1.0 equiv. Fe−**TCPPCl**	1.0: 1.0	4.4 ns

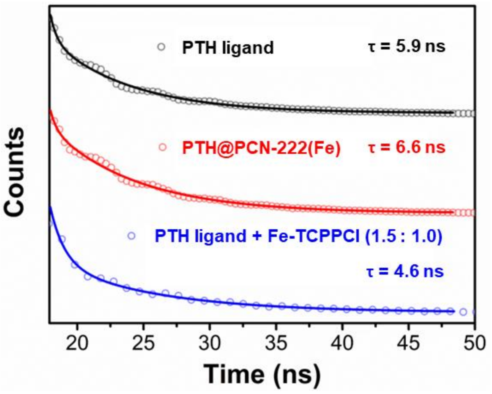

Fig. S9 Fluorescence lifetimes of **PTH** ligand, **PTH**@PCN−222(Fe), and the mixture of **PTH** ligand and Fe−**TCPPCl** (1.5:1.0) in DMF.

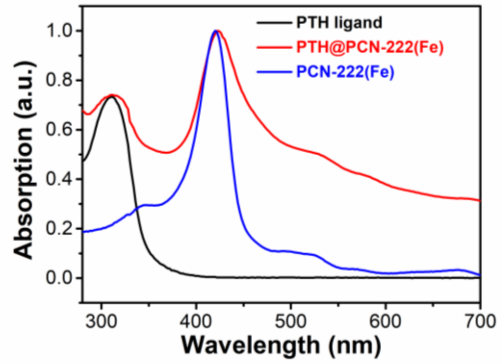

Fig. S10 The comparative UV-vis absorption spectra of **PTH** carboxylic ligand, PCN−222(Fe), and **PTH**@PCN−222(Fe) suspended in DMF.

4. Investigation on Photocatalytic Mechanism

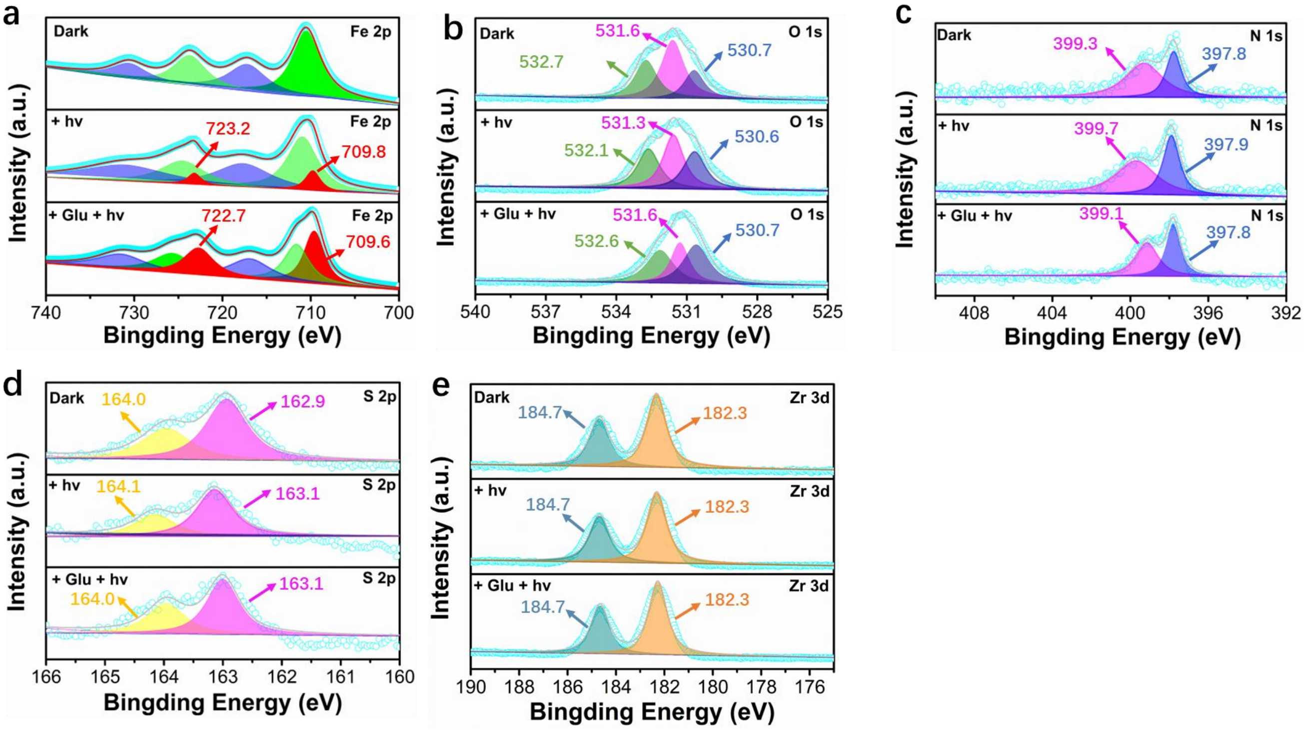

Fig. S11 XPS spectra of **PTH**@PCN−222(Fe) in the dark, after irradiation with a 365 nm LED, and after irradiation in the presence of glucose.

General Procedure for the Absorption of Guest Molecules in PTH@PCN−222(Fe)

10 mg **PTH**@PCN−222(Fe) was soaked in a methanol solution of 4-nitroacetophenone (**1k**) (0.1 M, 2 mL) overnight. The solid was then separated by centrifugation and rinsed with methanol to remove the substrate adsorbed on the surface. Then, the substrate encapsulated **PTH**@PCN−222(Fe) was subjected to FT-IR for the examination of potential host-guest behaviour (Fig. 3b).

5. DFT Calculation of PTH@PCN−222(Fe)

All the results were calculated using the spin-polarised DFT in the Dmol3 package.[4,5] The Perdew-Burke-Ernzerhof (PBE) was used to represent the exchange-correlation.[6] The relativistic effects of transition metal atoms were described using DFT semi-core pseudopotential (DSPP).[7] Convergence criteria for self-consistent field (SCF) calculations were set to 10^{-6} Hartrees for the total energy and electronic computations.

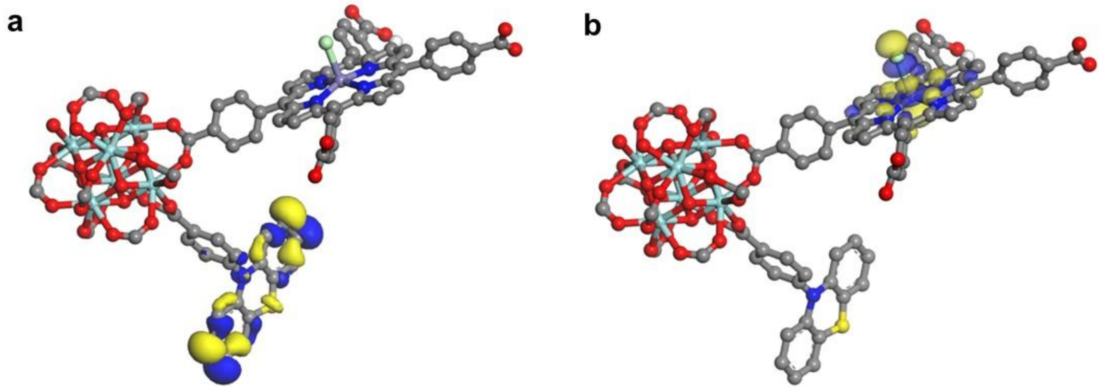

Fig. S12 Density functional theory (DFT) calculations of frontier orbitals (a) HOMO and (b) LUMO involved in photoexcitation of **PTH**@PCN−222(Fe).

6. Investigation on Continuous Photocatalysis of PTH@PCN−222(Fe)

General Procedure for Photocatalytic Reduction of Nitroarenes

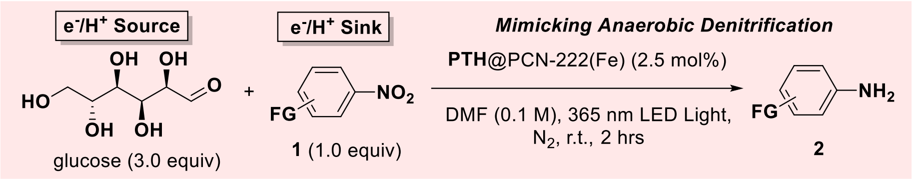

A 10 mL flame-dried Schlenk quartz flask was charged with a magnetic stir bar, **PTH**@PCN−222(Fe) (5.0 µmol, 0.025 equiv.), nitroarenes (0.2 mmol, 1.0 equiv.), glucose (0.6 mmol, 3.0 equiv.), and DMF (0.1 M, 2.0 mL). The resulting mixture was stirred and irradiated with a 365 nm LED under N_2 atmosphere at room temperature for 2 hrs. After the reaction, the photocatalyst was recovered by filtration. The filtrate was diluted with 20 mL of EtOAc and washed with deionised water three times. The organic phase was dried over anhydrous Na_2SO_4 and then concentrated under vacuum. The target products could be isolated through flash chromatography on silica gel.

General Procedure for Photocatalytic Oxidation of Amines to Imines

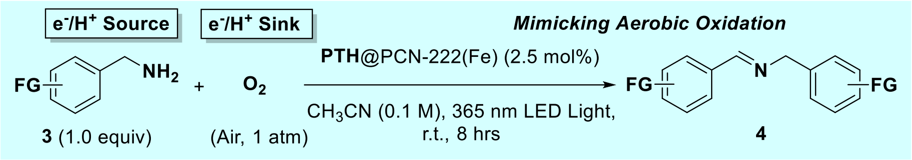

A 10 mL Schlenk quartz flask was charged with a magnetic stir bar, **PTH**@PCN−222(Fe) (5.0 µmol, 0.025 equiv.), benzylamine (0.2 mmol, 1.0 equiv.), and CH_3CN (0.1 M, 2.0 mL). The resulting mixture was stirred and irradiated with 365 nm LEDs in an air atmosphere for 8 hrs. After the reaction, the photocatalyst was recovered by filtration. The filtrate was diluted with 20 mL of EtOAc and washed with deionised water 3 times. The organic phase was dried over anhydrous Na_2SO_4 and then concentrated under vacuum. The target products could be isolated through flash chromatography on silica gel.

Kinetic Experiment of Photocatalytic Nitrobenzene Reduction

The reaction setup was similar to the aforementioned **General Procedure for Photocatalytic Reduction of Nitroarenes**, except for the two-time scale-up (nitrobenzene **1a**, 0.4 mmol, 1 equiv.) and the use of a specified photocatalyst. 0.1 mL of supernatant of the reaction mixture was taken by syringe for sampling at the specified time intervals. Conversion of substrate and yield of product were determined by GC-MS using 1,3,5-trimethoxybenzene as the internal standard (Figs. S11 and 3c).

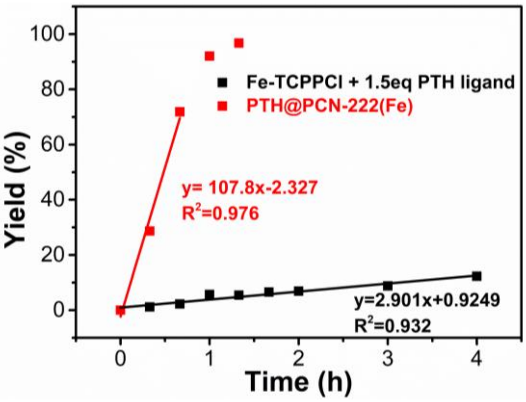

Fig. S13 The kinetic curve of nitrobenzene reduction catalysed by ligands (Fe−**TCPPCl** + 1.5 equiv. **PTH** ligand) and **PTH**@PCN−222(Fe) under standard conditions. GC yields were determined by using 1,3,5-trimethoxybenzene as the internal standard.

Recycling catalytic experiments of photocatalytic nitrobenzene reduction

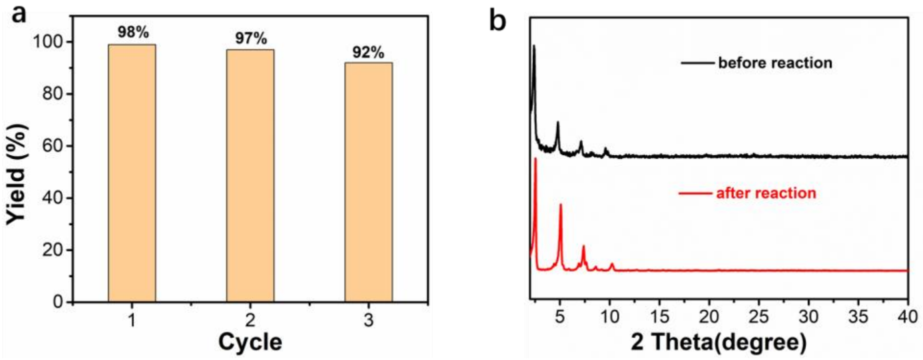

Fig. S14 (a) Histogram of recycling catalytic experiments for photocatalytic nitrobenzene reduction using **PTH**@PCN−222(Fe). (b) PXRD patterns of as-synthesized **PTH**@PCN−222(Fe) and the recycled catalyst after reactions.

7. NMR Data and Spectra of the Isolated Compounds

Aniline (**2a**)

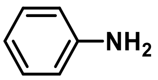

^{1}H NMR (400 MHz, CDCl$_3$): δ 7.07 (t, J = 7.4 Hz, 2H), 6.68 (t, J = 7.3, 6.8 Hz, 1H), 6.60 (d, J = 8.1 Hz, 2H), 3.36 (br s, 2H); ^{13}C NMR (101 MHz, CDCl$_3$) δ 146.41 (s), 129.22 (s), 118.41 (s), 115.06 (s). Spectral data match those previously reported in the literature.[8]

p-Toluidine (**2b**)

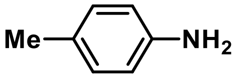

^{1}H NMR (400 MHz, CDCl$_3$): δ 6.88 (d, J = 7.9 Hz, 2H), 6.52 (d, J = 8.1 Hz, 2H), 3.32 (br s, 2H), 2.16 (s, 3H); ^{13}C NMR (101 MHz, CDCl$_3$): δ 143.86 (s), 129.85 (s), 127.91 (s), 115.39 (s), 20.55 (s). Spectral data match those previously reported in the literature.[9]

4-Methoxyaniline (**2c**)

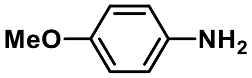

^{1}H NMR (400 MHz, CDCl$_3$): δ 6.67 (d, J = 8.5 Hz, 2H), 6.57 (d, J = 8.5 Hz, 2H), 3.66 (s, 3H), 3.16 (br s, 2H); ^{13}C NMR (101 MHz, CDCl$_3$): δ 152.92 (s), 140.01 (s), 116.55 (s), 114.92 (s), 55.84 (s). Spectral data match those previously reported in the literature.[10]

4-Aminophenol (**2d**)

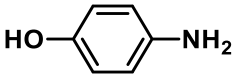

^{1}H NMR (400 MHz, DMSO-d_6): δ 8.28 (d, J = 80.1 Hz, 1H), 6.45 – 6.42 (m, 4H), 4.32 (br s, 2H); ^{13}C NMR (101 MHz, DMSO): δ 153.5 (s), 145.8 (s), 120.8 (s), 120.5 (s). Spectral data match those previously reported in the literature.[10]

4-(*tert*-Butyl)aniline (**2e**)

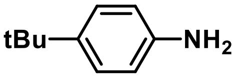

^{1}H NMR (400 MHz, CDCl$_3$): δ 7.11 (d, J = 8.5 Hz, 2H), 6.58 (d, J = 8.5 Hz, 2H), 3.36 (br s, 2H), 1.22 (s, 9H); ^{13}C NMR (101 MHz, CDCl$_3$): δ 143.88 (s), 141.44 (s), 126.11 (s), 115.01 (s), 33.97 (s), 31.62 (s). Spectral data match those previously reported in the literature.[11]

4-Fluoroaniline (**2f**)

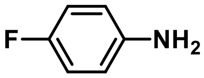

^{1}H NMR (400 MHz, CDCl$_3$): δ 6.78 (app. t, J = 8.7 Hz, 2H), 6.55 (dd, J = 8.7, 4.4 Hz, 2H), 3.45 (br s, 2H); ^{13}C NMR (101 MHz, CDCl$_3$): δ 156.46 (d, J = 235.4 Hz), 142.53 (d, J = 1.7 Hz), 116.12 (d, J = 7.4 Hz), 115.71 (d, J = 22.4 Hz). Spectral data match those previously reported in the literature.[12]

4-Chloroaniline (**2g**)

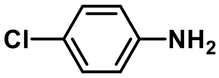

^{1}H NMR (400 MHz, CDCl$_3$): δ 7.02 (d, J = 8.5 Hz, 2H), 6.53 (d, J = 8.5 Hz, 2H), 3.45 (br s, 2H). ^{13}C NMR (101 MHz, CDCl$_3$): δ 145.06 (s), 129.21 (s), 123.24 (s), 116.34 (s). Spectral data match those previously reported in the literature.[12]

4-Bromoaniline (**2h**)

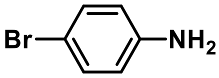

^{1}H NMR (400 MHz, CDCl$_3$): δ 7.15 (d, J = 8.6 Hz, 2H), 6.47 (d, J = 8.6 Hz, 2H), 3.50 (s, 2H); ^{13}C NMR (101 MHz, CDCl$_3$): δ 145.52 (s), 132.11 (s), 116.83 (s), 110.31 (s). Spectral data match those previously reported in the literature.[12]

3-Bromoaniline (**2i**)

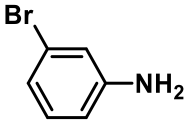

^{1}H NMR (400 MHz, CDCl$_3$): δ 6.92 (t, J = 7.9 Hz, 1H), 6.83 – 6.68 (m, 2H), 6.50 (dd, J = 8.0, 1.1 Hz, 1H), 3.58 (br s, 2H); ^{13}C NMR (101 MHz, CDCl$_3$): δ 147.91 (s), 130.71 (s), 123.15 (s), 121.47 (s), 117.93 (s), 113.74 (s). Spectral data match those previously reported in the literature.[11]

2-Bromoaniline (**2j**)

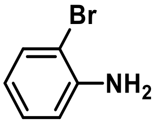

^{1}H NMR (400 MHz, CDCl$_3$): δ 7.32 (t, J = 14.1 Hz, 1H), 7.04 (t, J = 7.6 Hz, 1H), 6.71 (d, J = 7.0 Hz, 1H), 6.55 (t, J = 7.2 Hz, 1H); ^{13}C NMR (101 MHz, CDCl$_3$): δ 144.19 (s), 132.70 (s), 128.45 (s), 119.53 (s), 115.88 (s), 109.45. Spectral data match those previously reported in the literature.[12]

1-(4-Aminophenyl)ethan-1-one (**2k**)

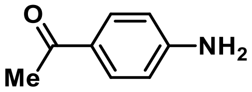

^{1}H NMR (400 MHz, CDCl$_3$): δ 7.72 (d, J = 7.1 Hz, 2H), 6.56 (d, J = 7.2 Hz, 2H), 4.03 (br s, 2H), 2.42 (s, 3H); ^{13}C NMR (101 MHz, CDCl$_3$): δ 196.70 (s), 151.33 (s), 130.91 (s), 127.87 (s), 113.81 (s), 26.17 (s). Spectral data match those previously reported in the literature.[12]

Methyl 4-aminobenzoate (**2l**)

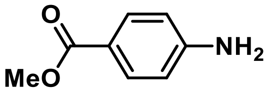

^{1}H NMR (400 MHz, CDCl$_3$): δ 7.82 (dd, J = 44.2, 8.4 Hz, 2H), 6.56 (d, J = 8.5 Hz, 2H), 3.98 (br s, 2H), 3.77 (s, 3H); ^{13}C NMR (101 MHz, CDCl$_3$): δ 167.30 (s), 151.02 (s), 131.69 (s), 119.74 (s), 113.88 (s), 51.68 (s). Spectral data match those previously reported in the literature.[11]

4-Aminobenzonitrile (**2m**)

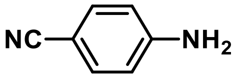

^{1}H NMR (400 MHz, CDCl$_3$): δ 7.33 (d, J = 8.5 Hz, 2H), 6.57 (d, J = 8.5 Hz, 2H), 4.12 (br s, 2H). ^{13}C NMR (101 MHz, CDCl$_3$): δ 150.66 (s), 133.83 (s), 120.33 (s), 114.48 (s), 99.88 (s). Spectral data match those previously reported in the literature.[11]

Quinolin-6-amine (**2n**)

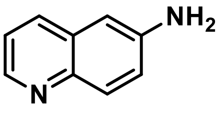

^{1}H NMR (400 MHz, CDCl$_3$): δ 8.65 – 8.45 (m, 1H), 7.82 (t, J = 9.7 Hz, 2H), 7.18 (dd, J = 8.2, 4.1 Hz, 1H), 7.07 (dd, J = 8.9, 2.4 Hz, 1H), 6.80 (d, J = 2.3 Hz, 1H), 3.71 (br s, 2H); ^{13}C NMR (101 MHz, CDCl$_3$): δ 146.82 (s), 144.79 (s), 143.49 (s), 133.82 (s), 130.56 (s), 129.87 (s), 121.65 (s), 121.44 (s), 107.43 (s). Spectral data match those previously reported in the literature.[13]

4-Vinylaniline (**2o**)

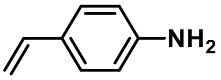

^{1}H NMR (400 MHz, $CDCl_3$): δ 7.12 (d, *J* = 8.3 Hz, 2H), 6.60 – 6.44 (m, 3H), 5.45 (d, *J* = 17.6 Hz, 1H), 4.94 (d, *J* = 10.9 Hz, 1H), 3.52 (s, 2H); ^{13}C NMR (101 MHz, $CDCl_3$): δ 146.28 (s), 136.61 (s), 128.33 (s), 127.40 (s), 115.05 (s), 110.03 (s). Spectral data match those previously reported in the literature.[9]

(*E*)-*N*-benzyl-1-phenylmethanimine (**4a**)

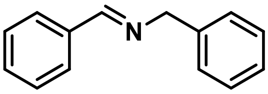

^{1}H NMR (400 MHz, $CDCl_3$): δ 8.30 (s, 1H), 7.75 – 7.65 (m, 2H), 7.37 – 7.29 (m, 3H), 7.27 – 7.21 (m, 4H), 7.17 (dd, *J* = 8.5, 4.4 Hz, 1H), 4.73 (s, 2H); ^{13}C NMR (101 MHz, $CDCl_3$): δ 162.05 (s), 139.41 (s), 136.28 (s), 130.84 (s), 128.69 (s), 128.58 (s), 128.37 (s), 128.07 (s), 127.07 (s), 65.14 (s). Spectral data match those previously reported in the literature.[14]

(*E*)-*N*-(4-methylbenzyl)-1-(p-tolyl)methanimine (**4b**)

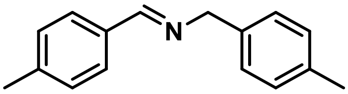

^{1}H NMR (400 MHz, $CDCl_3$): δ 8.24 (s, 1H), 7.57 (d, *J* = 7.8 Hz, 2H), 7.12 (t, *J* = 6.4 Hz, 4H), 7.05 (d, *J* = 7.7 Hz, 2H), 4.67 (s, 2H), 2.28 (s, 3H), 2.24 (s, 3H); ^{13}C NMR (101 MHz, $CDCl_3$): δ 161.76 (s), 141.04 (s), 136.57 (s), 136.45 (s), 133.72 (s), 129.38 (s), 129.24 (s), 128.33 (s), 128.04 (s), 64.89 (s), 21.59 (s), 21.19 (s). Spectral data match those previously reported in the literature.[15]

Methyl (*E*)-4-(((4-(methoxycarbonyl)benzyl)imino)methyl)benzoate (**4c**)

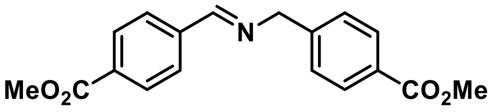

^{1}H NMR (400 MHz, $CDCl_3$) δ 8.35 (s, 1H), 8.06 – 7.95 (m, 2H), 7.93 (d, *J* = 8.0 Hz, 2H), 7.73 (dd, *J* = 26.4, 8.2 Hz, 2H), 7.33 (d, *J* = 8.0 Hz, 2H), 4.79 (s, 2H), 3.83 (s, 3H), 3.81 (s, 3H). ^{13}C NMR (101 MHz, $CDCl_3$) δ 167.01 (s), 166.62 (s), 161.63 (s), 144.32 (s), 139.84 (s), 132.14 (s), 129.95 (s), 129.92 (s), 129.02 (s), 128.23 (s), 127.85 (s), 64.72 (s), 52.33 (s), 52.12 (s). Spectral data match those previously reported in the literature.[16]

(*E*)-*N*-(4-(*tert*-butyl)benzyl)-1-(4-(*tert*-butyl)phenyl)methanimine (**4d**)

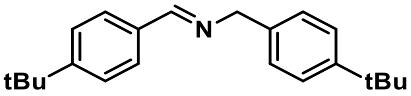

^{1}H NMR (400 MHz, CDCl$_3$): *δ* 8.35 (s, 1H), 8.00 (d, *J* = 8.0 Hz, 2H), 7.93 (d, *J* = 8.0 Hz, 2H), 7.76 (d, *J* = 8.1 Hz, 2H), 7.33 (d, *J* = 8.0 Hz, 2H), 4.79 (s, 2H), 3.83 (s, 9H), 3.81 (s, 9H); ^{13}C NMR (101 MHz, CDCl$_3$): *δ* 161.68 (s), 154.10 (s), 149.79 (s), 136.54 (s), 133.67 (s), 128.16 (s), 127.75 (s), 125.57 (s), 125.42 (s), 64.87 (s), 31.47 (s), 31.30 (s). Spectral data match those previously reported in the literature.[17]

(*E*)-*N*-(4-chlorobenzyl)-1-(4-chlorophenyl)methanimine (**4e**)

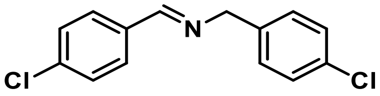

^{1}H NMR (400 MHz, CDCl$_3$): *δ* 8.21 (s, 1H), 7.59 (d, *J* = 8.4 Hz, 2H), 7.27 (d, *J* = 8.3 Hz, 2H), 7.18 (dd, *J* = 21.3, 8.4 Hz, 4H), 4.65 (s, 2H); ^{13}C NMR (101 MHz, CDCl$_3$): *δ* 160.87 (s), 137.73 (s), 136.93 (s), 134.55 (s), 132.87 (s), 129.54 (s), 129.34 (s), 128.99 (s), 128.71 (s), 64.22 (s). Spectral data match those previously reported in the literature.[17]

(*E*)-*N*-(4-bromobenzyl)-1-(4-bromophenyl)methanimine (**4f**)

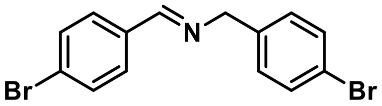

^{1}H NMR (400 MHz, CDCl$_3$): *δ* 8.23 (s, 1H), 7.55 (d, *J* = 8.2 Hz, 2H), 7.46 (d, *J* = 8.2 Hz, 2H), 7.38 (d, *J* = 8.1 Hz, 2H), 7.12 (d, *J* = 8.0 Hz, 2H), 4.65 (s, 2H); ^{13}C NMR (101 MHz, CDCl$_3$): *δ* 161.08 (s), 138.21 (s), 134.98 (s), 132.01 (s), 131.71 (s), 129.79 (s), 129.75 (s), 125.47 (s), 121.04 (s), 64.33 (s). Spectral data match those previously reported in the literature.[17]

^{1}H and ^{13}C NMR Spectra of Aniline(**2a**)

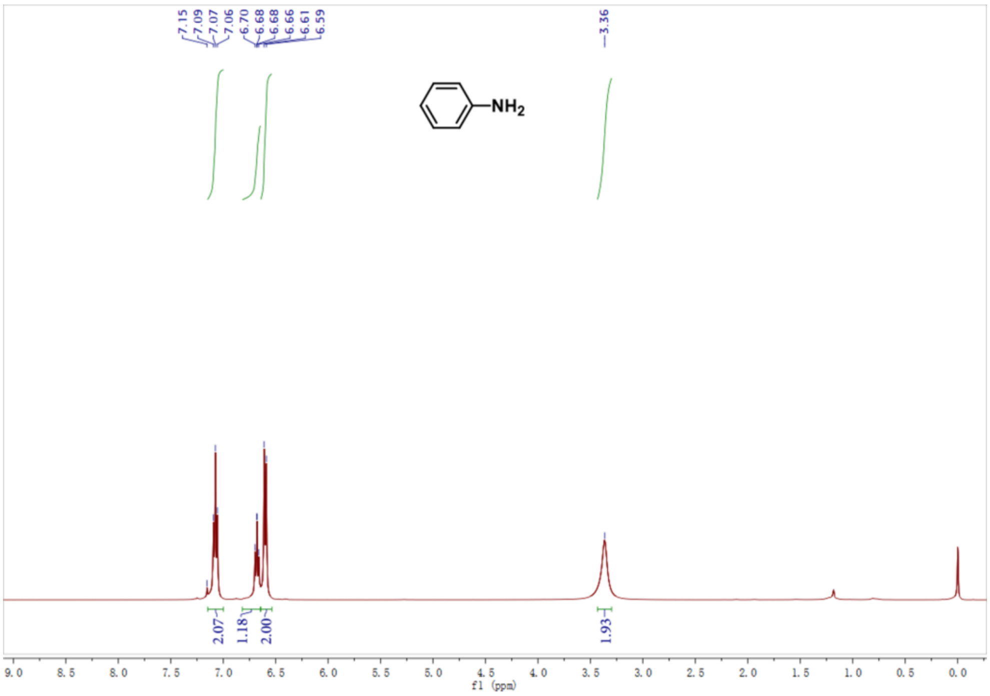

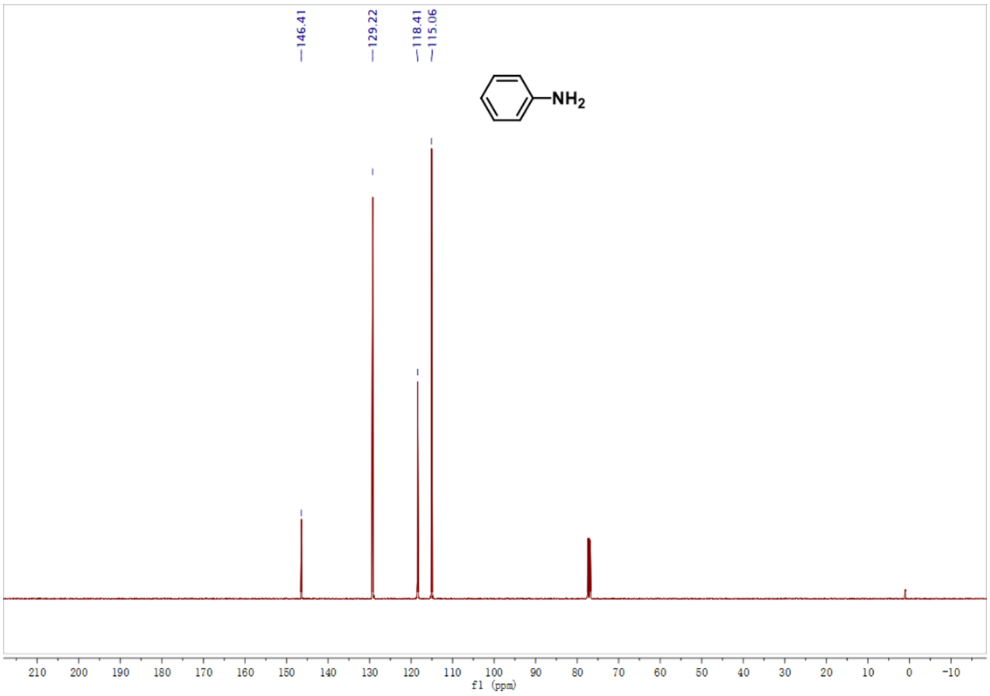

^{1}H and ^{13}C NMR Spectra of *p*-Toluidine (**2b**)

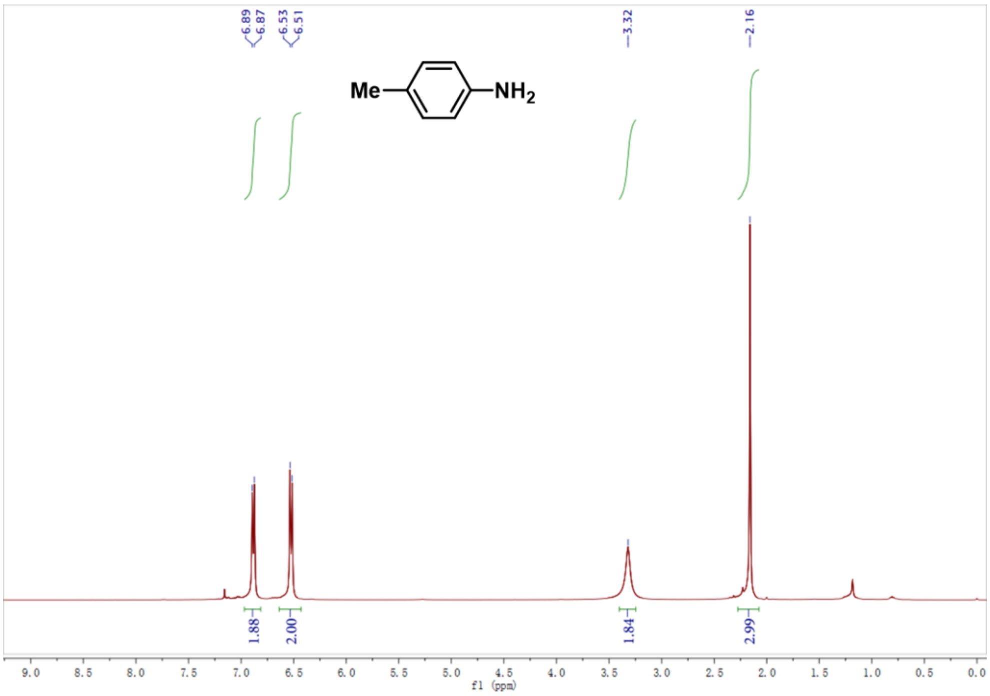

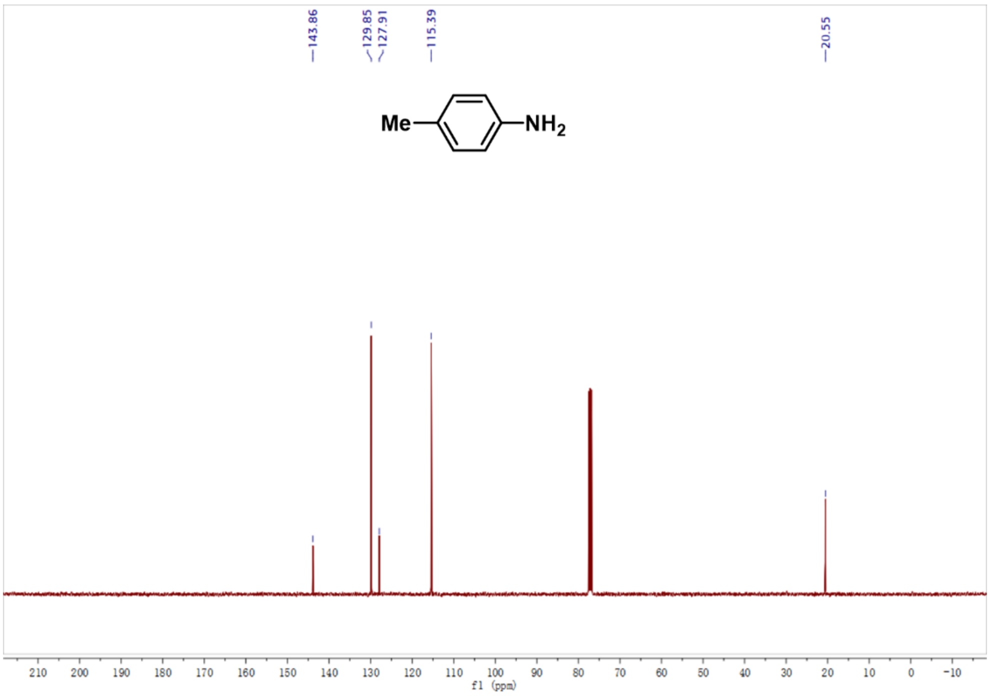

^{1}H and ^{13}C NMR Spectra of 4-Methoxyaniline (**2c**)

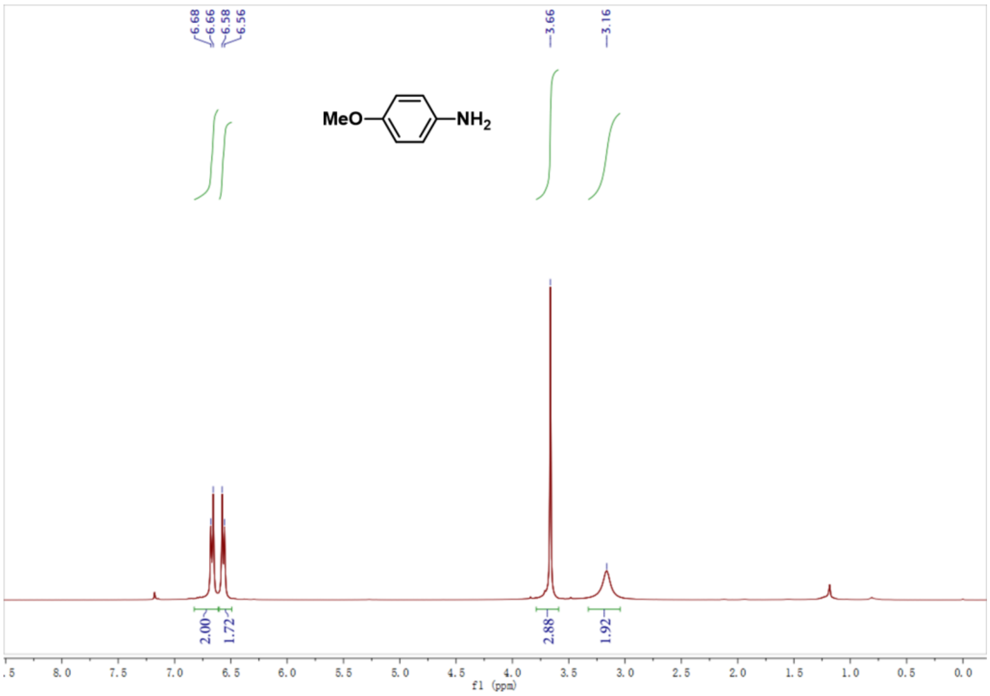

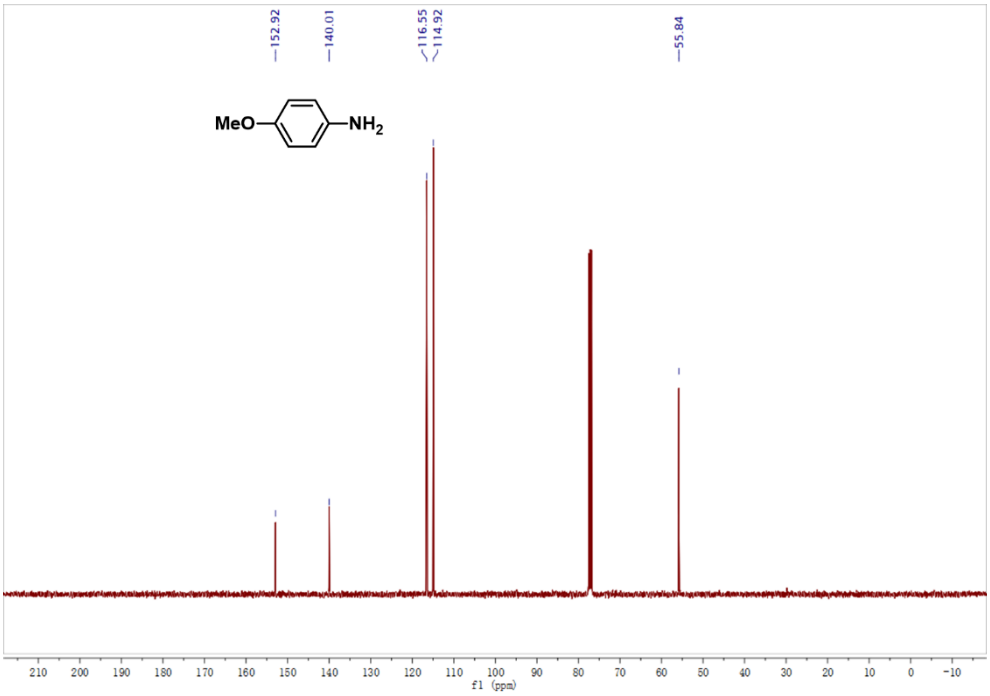

^{1}H and ^{13}C NMR Spectra of 4-Aminophenol (**2d**)

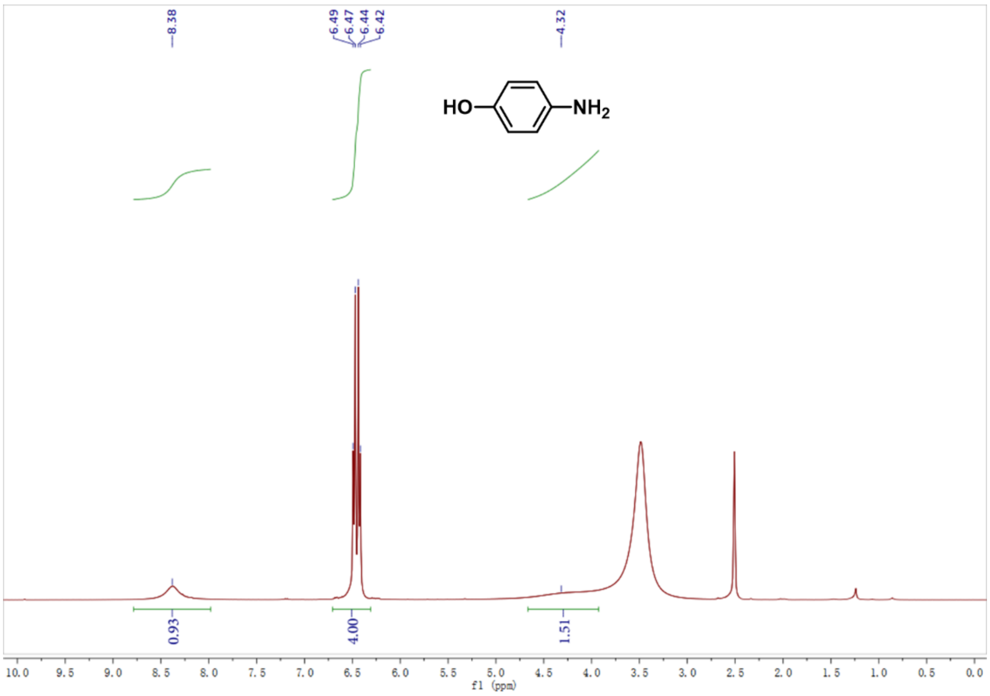

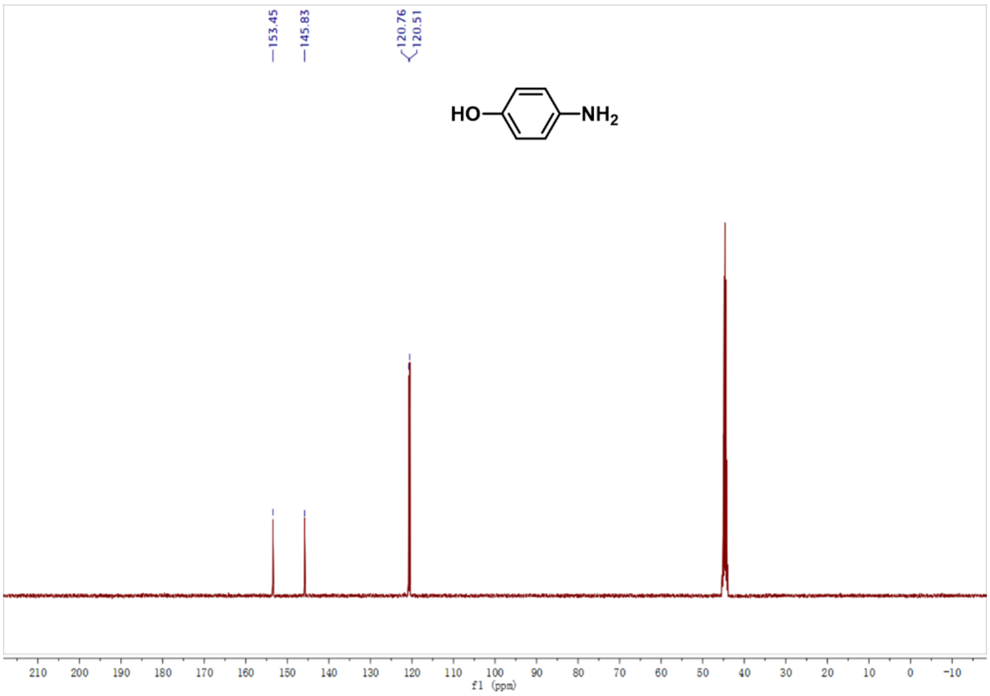

^{1}H and ^{13}C NMR Spectra of 4-(*tert*-butyl)aniline (**2e**)

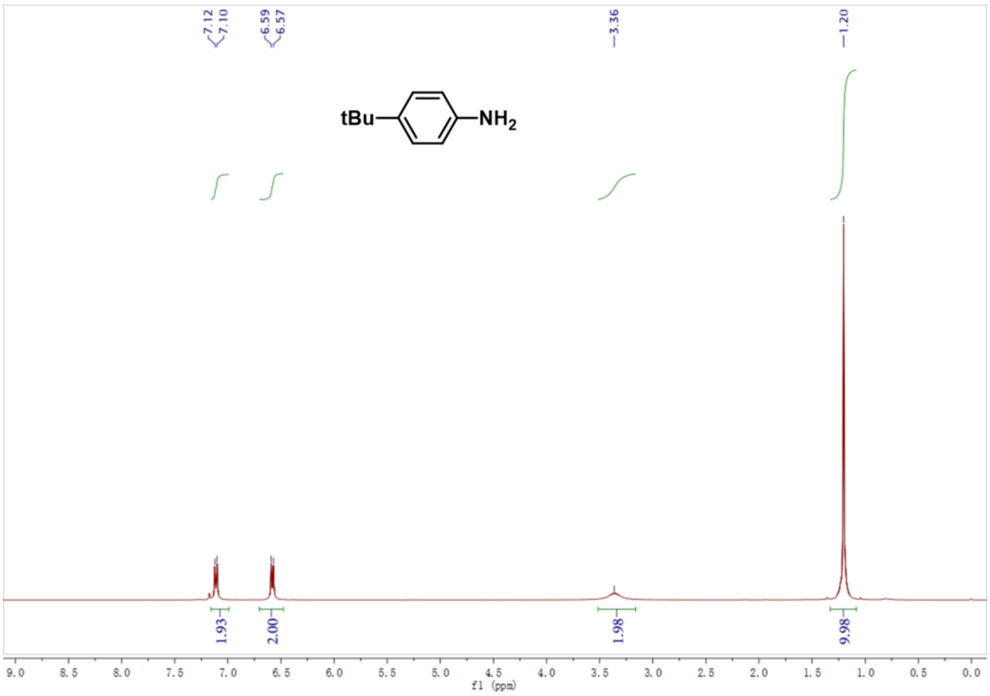

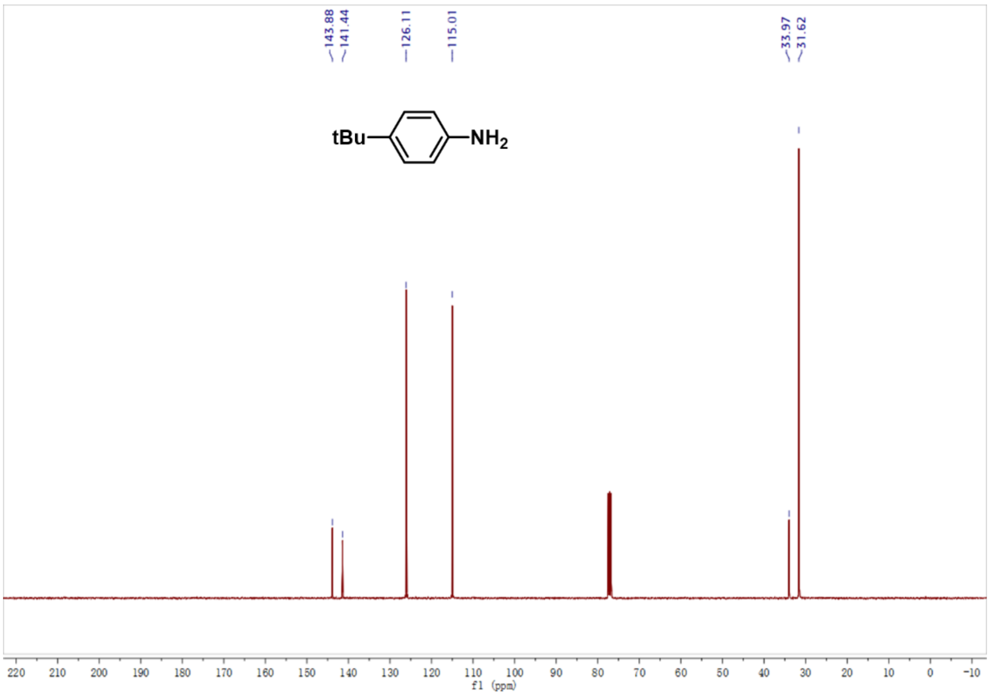

^{1}H and ^{13}C NMR Spectra of 4-Fluoroaniline (**2f**)

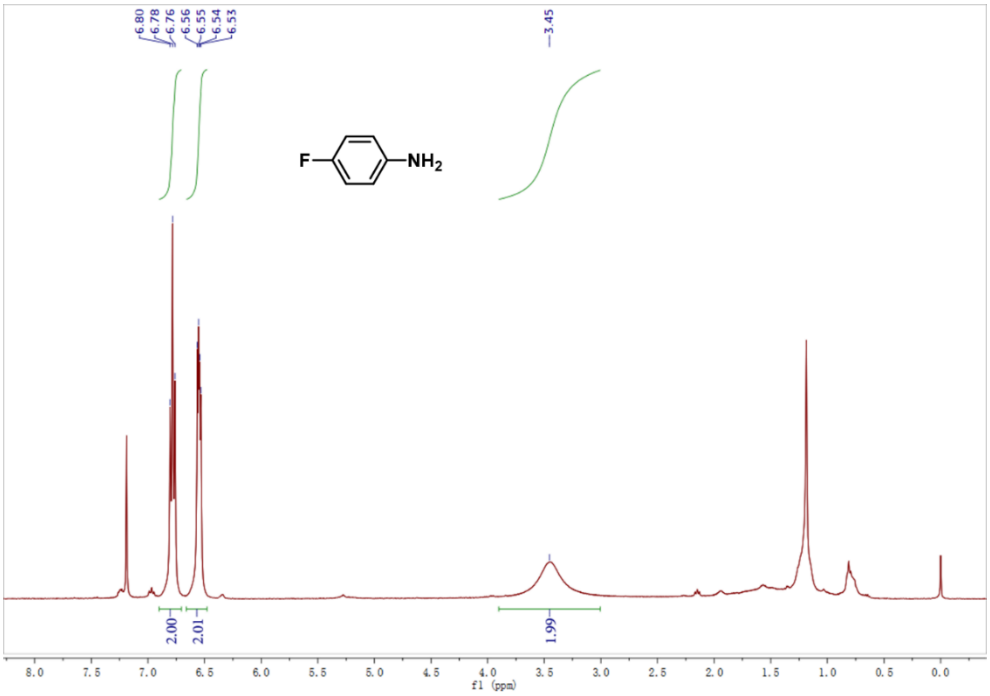

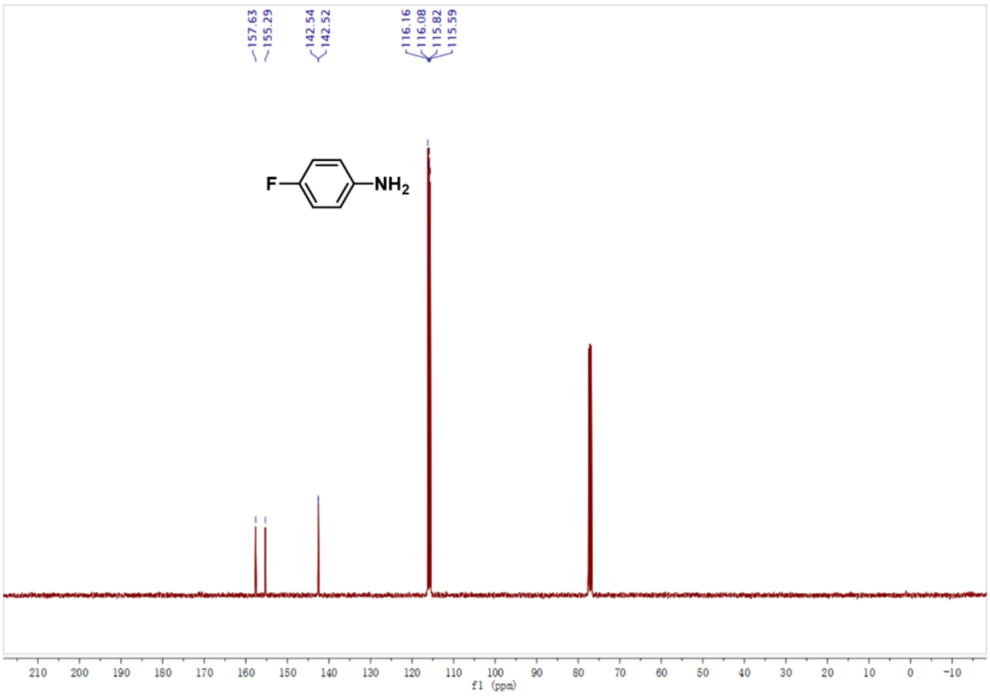

^{1}H and ^{13}C NMR Spectra of 4-Chloroaniline (**2g**)

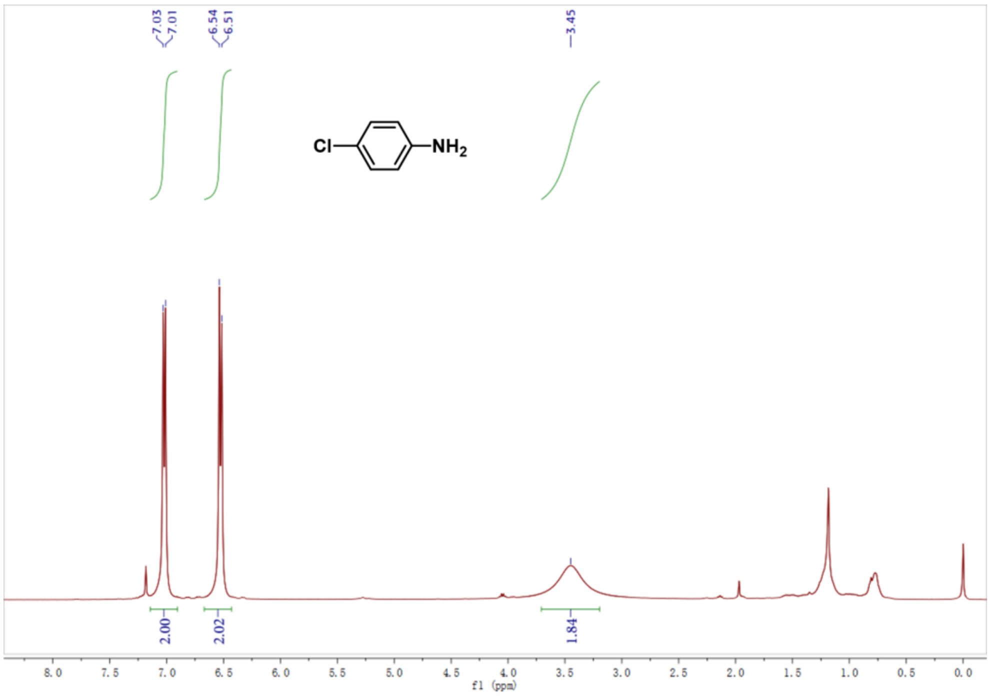

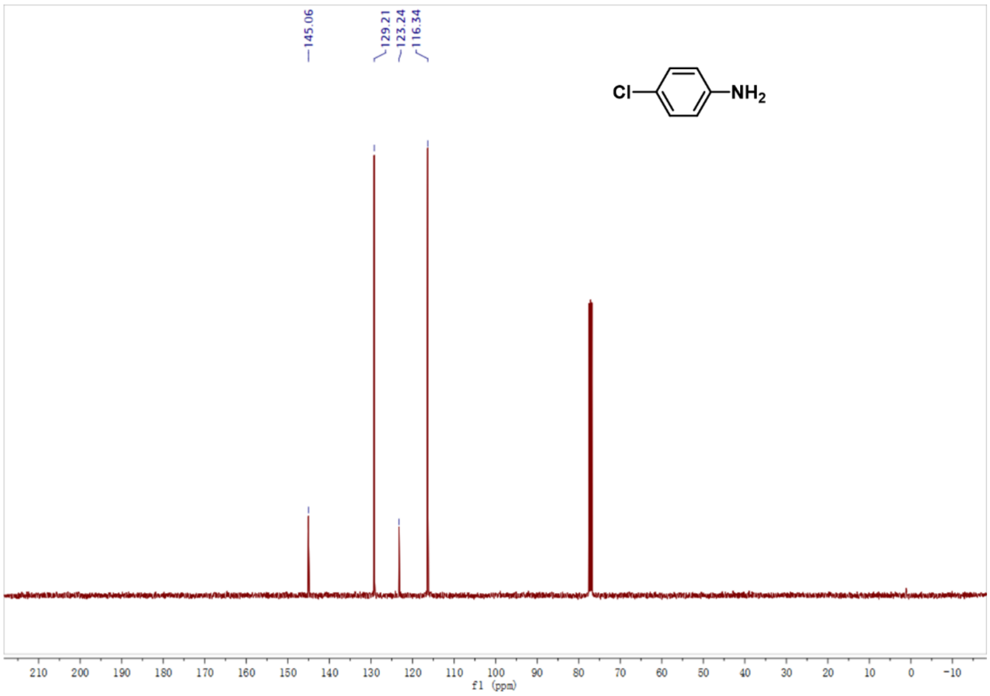

^{1}H and ^{13}C NMR Spectra of 4-Bromoaniline (**2h**)

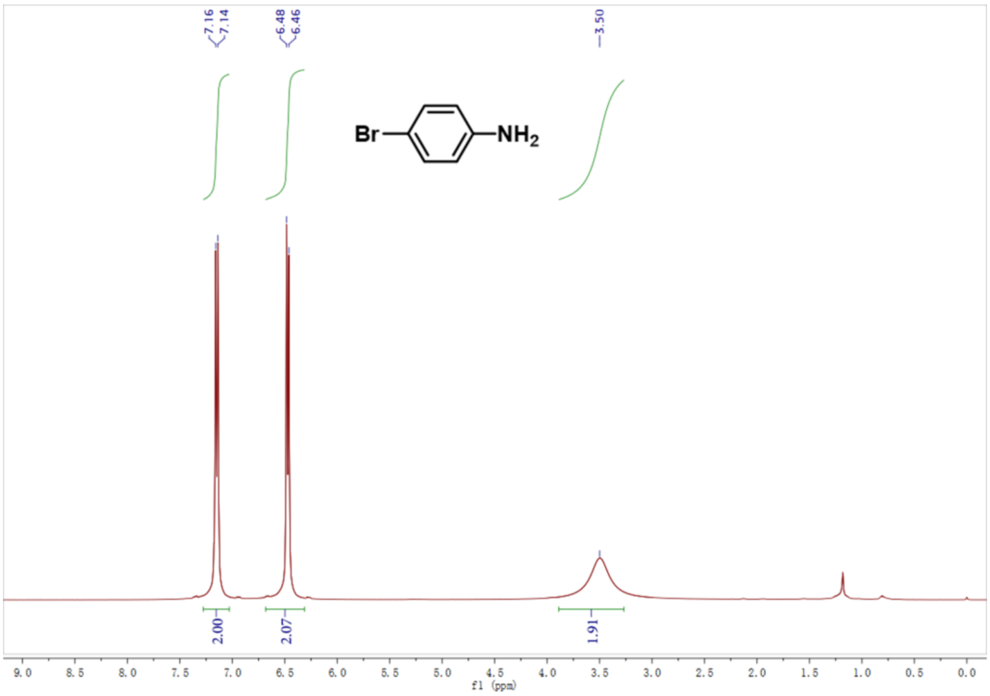

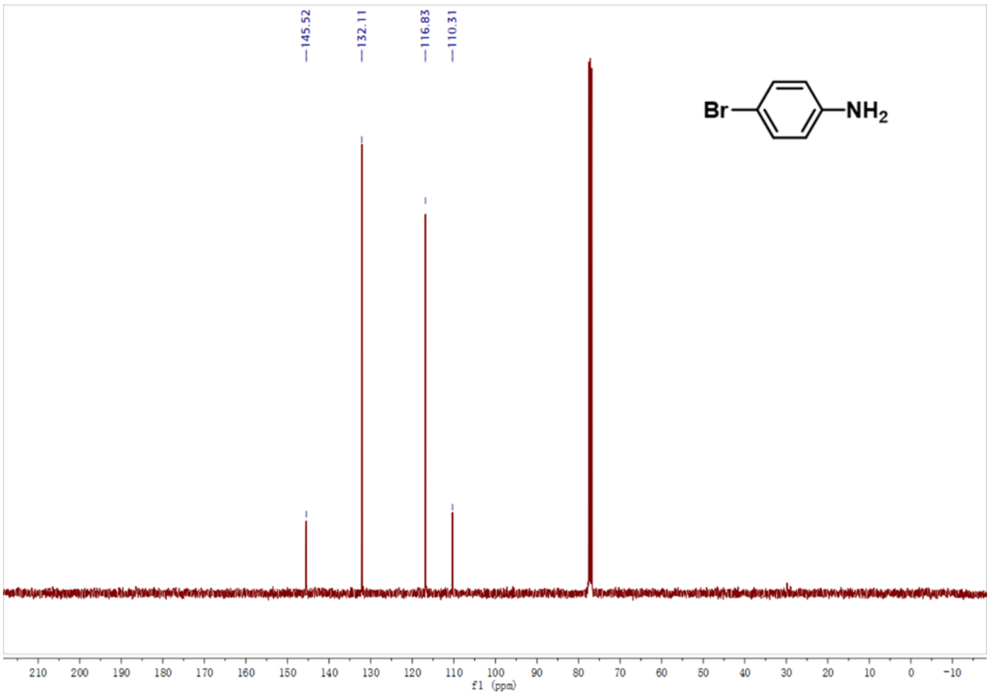

^{1}H and ^{13}C NMR Spectra of 3-Bromoaniline (**2i**)

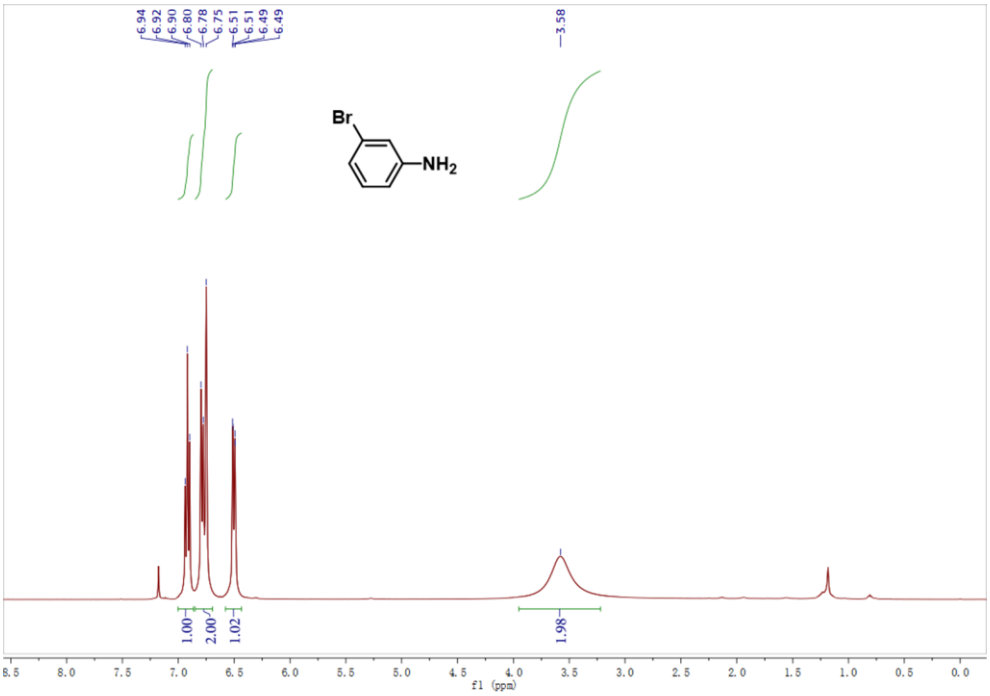

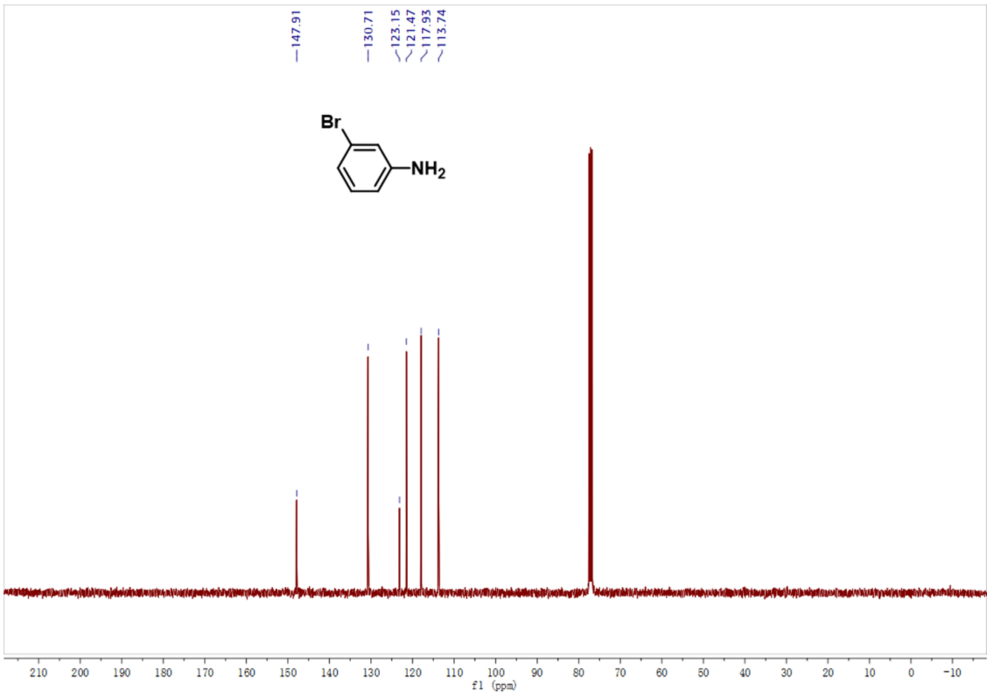

^{1}H and ^{13}C NMR Spectra of 2-Bromoaniline (**2j**)

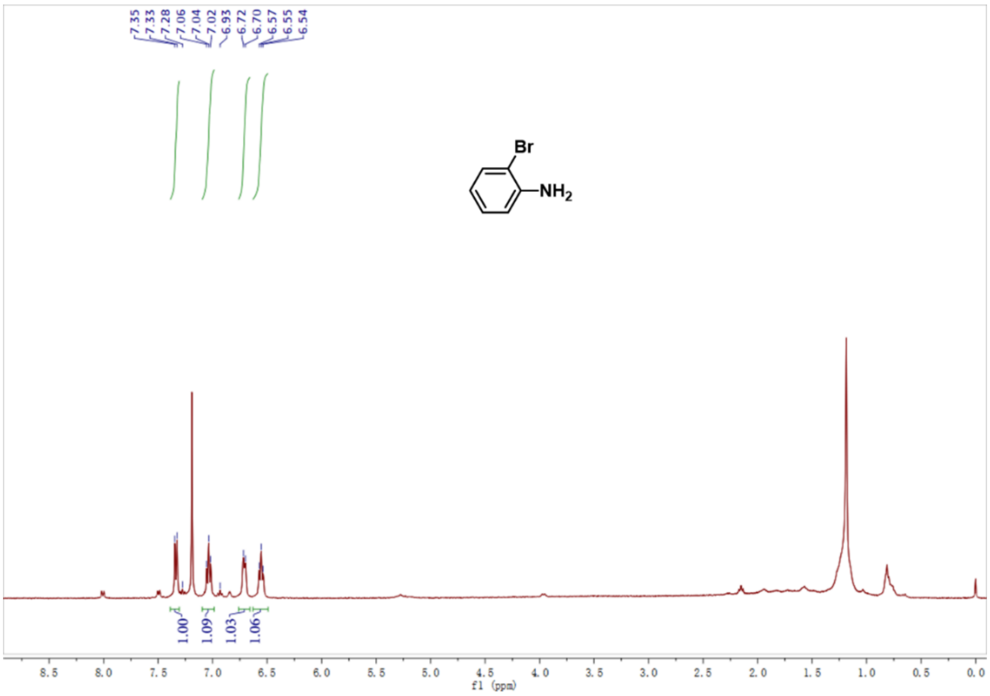

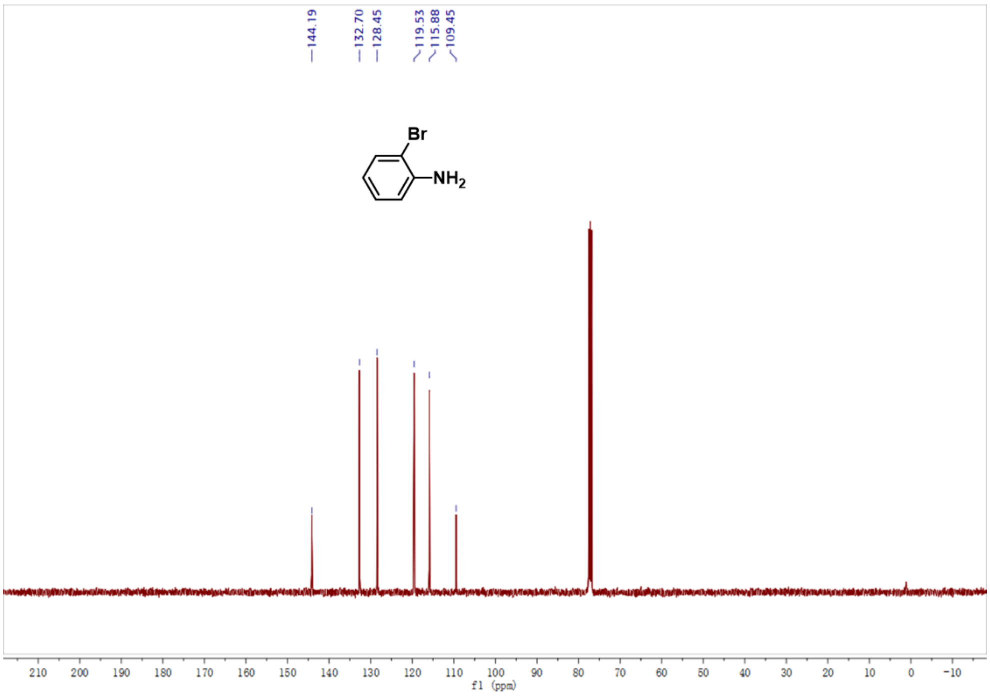

^1H and ^{13}C NMR Spectra of 1-(4-Aminophenyl)ethan-1-one (**2k**)

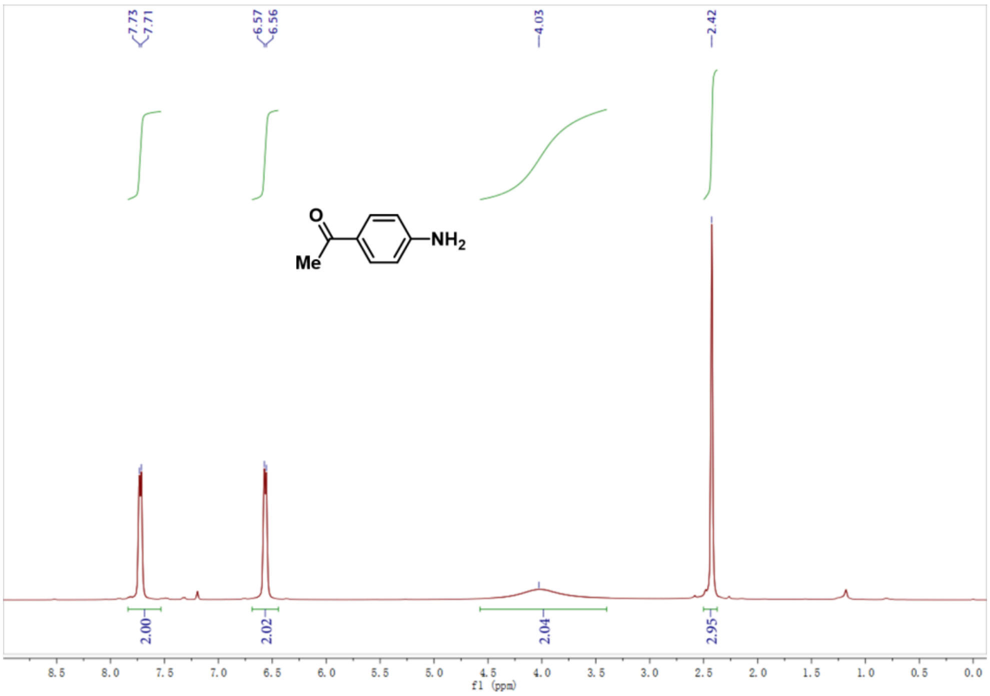

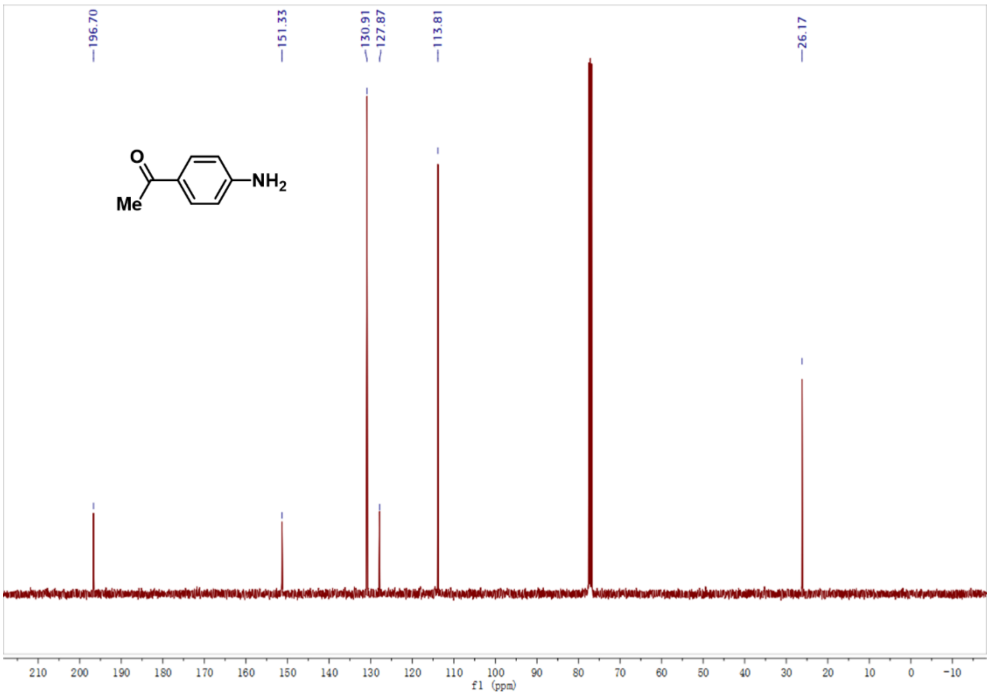

^{1}H and ^{13}C NMR Spectra of methyl 4-Aminobenzoate (**2l**)

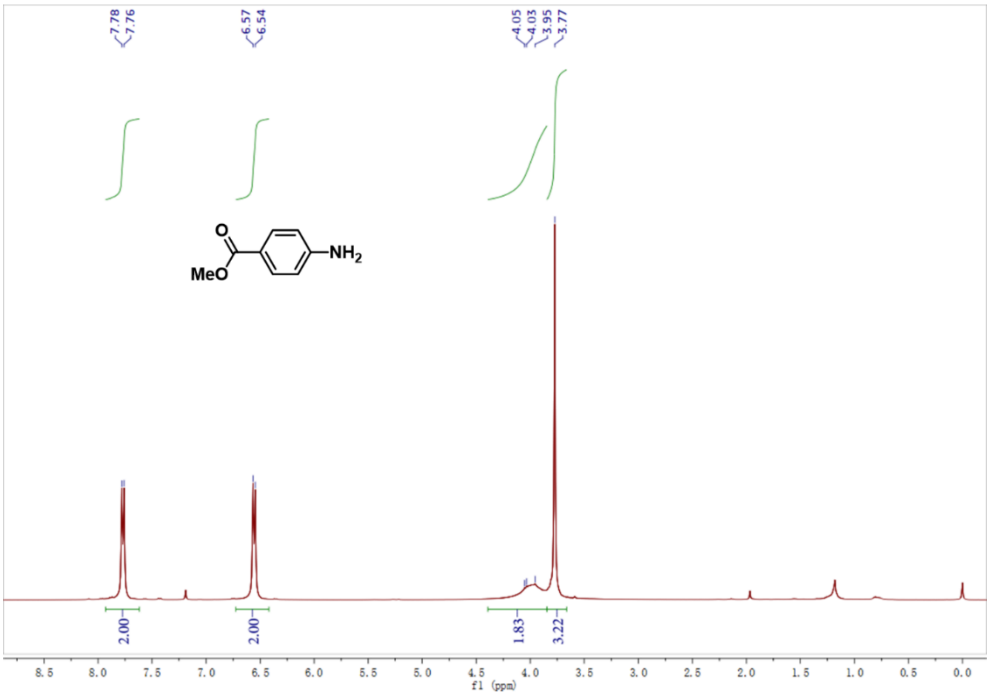

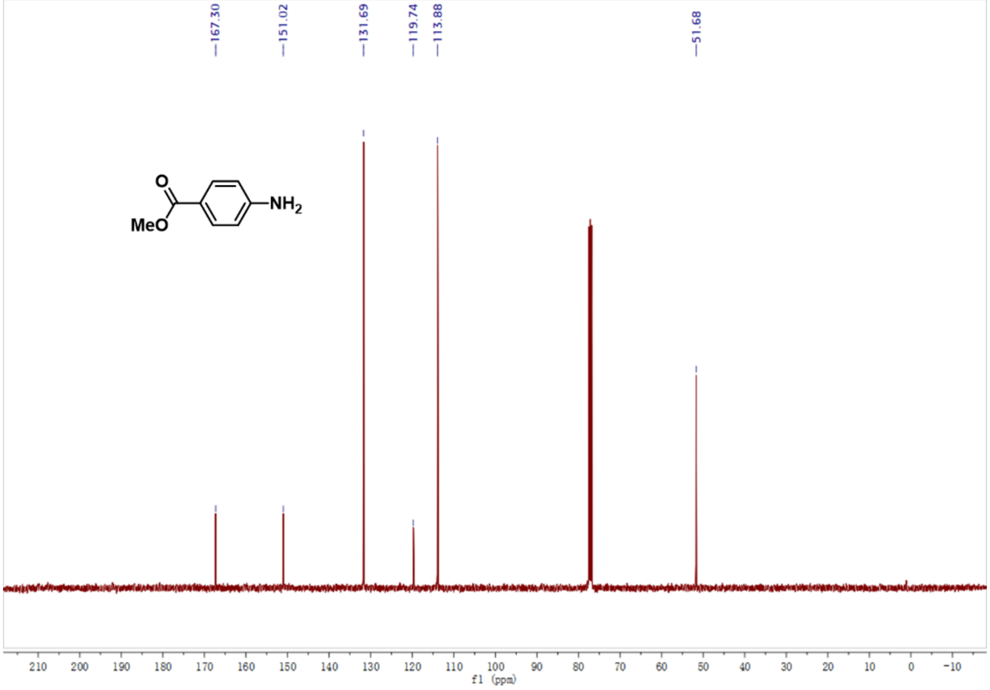

^1H and ^{13}C NMR Spectra of 4-Aminobenzonitrile (**2m**)

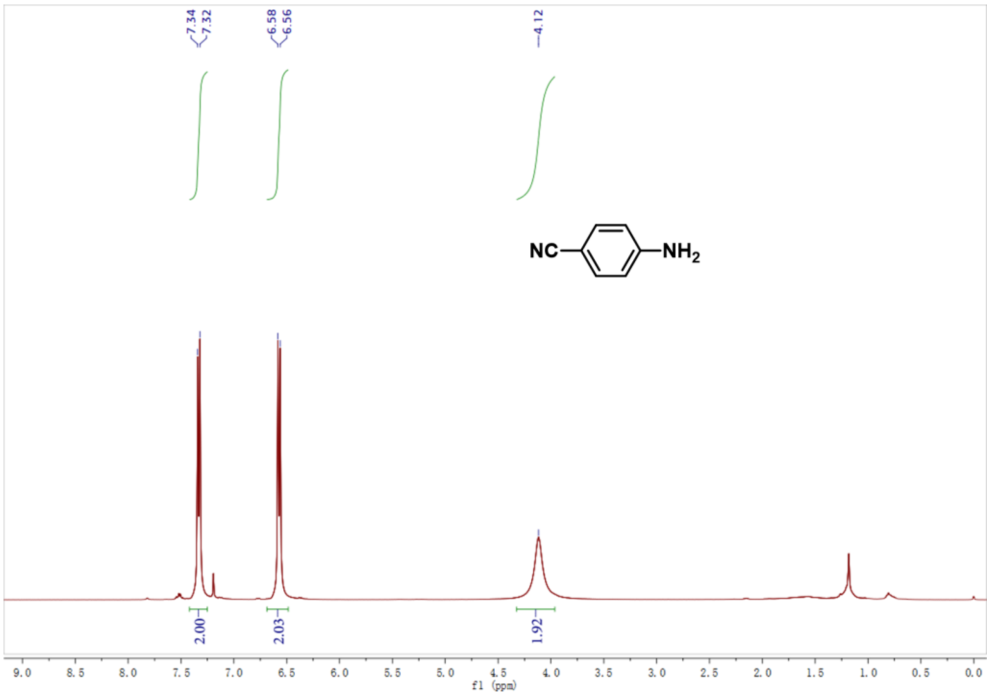

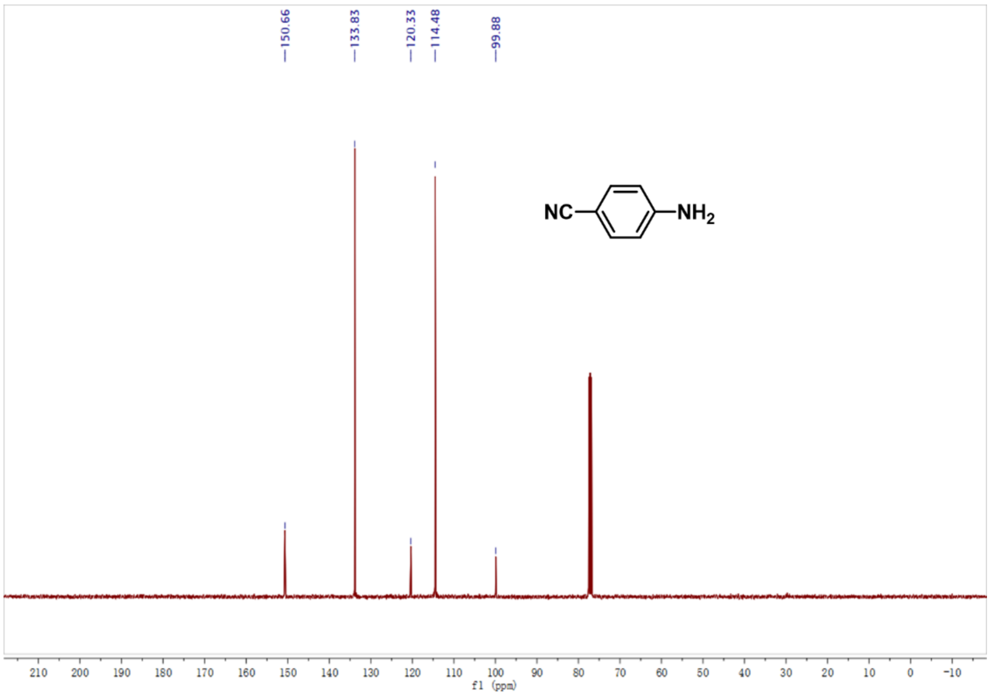

^{1}H and ^{13}C NMR Spectra of Quinolin-6-amine (**2n**)

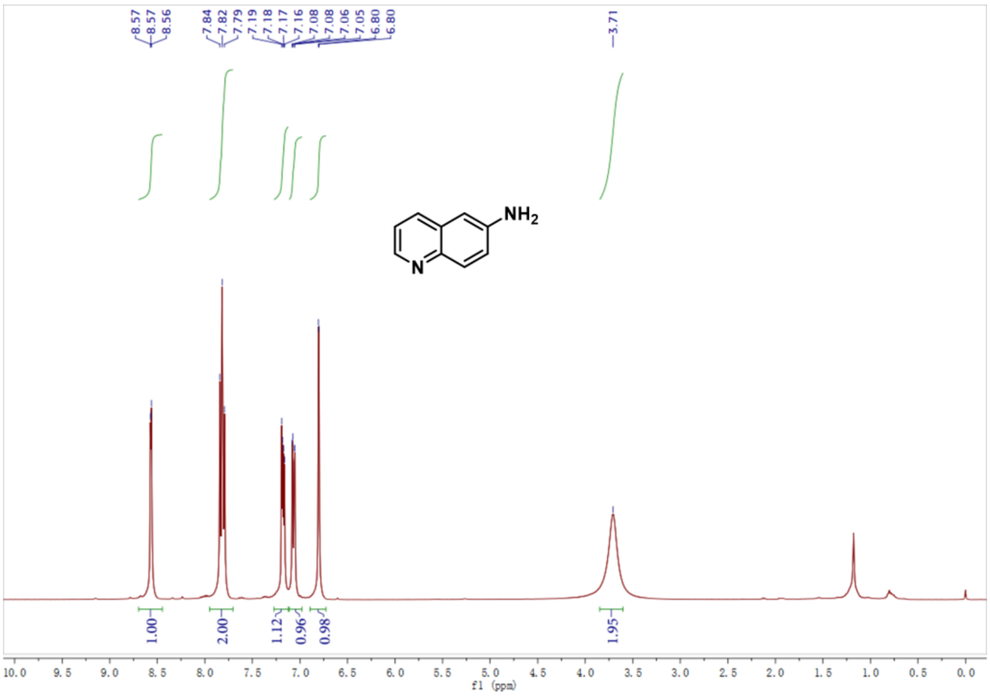

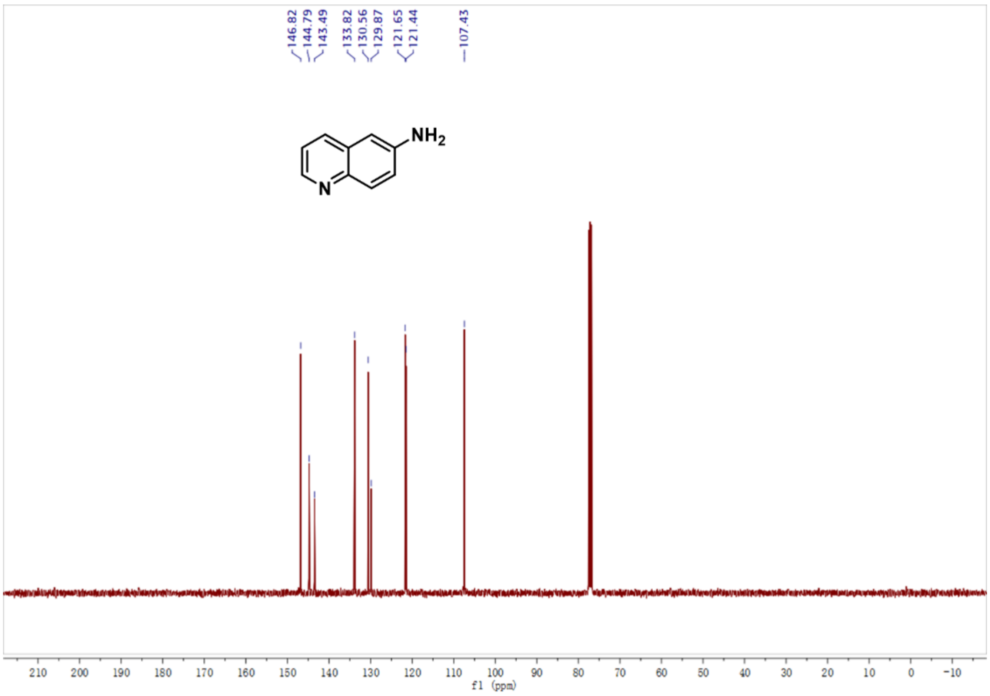

^{1}H and ^{13}C NMR Spectra of 4-Vinylaniline (**2o**)

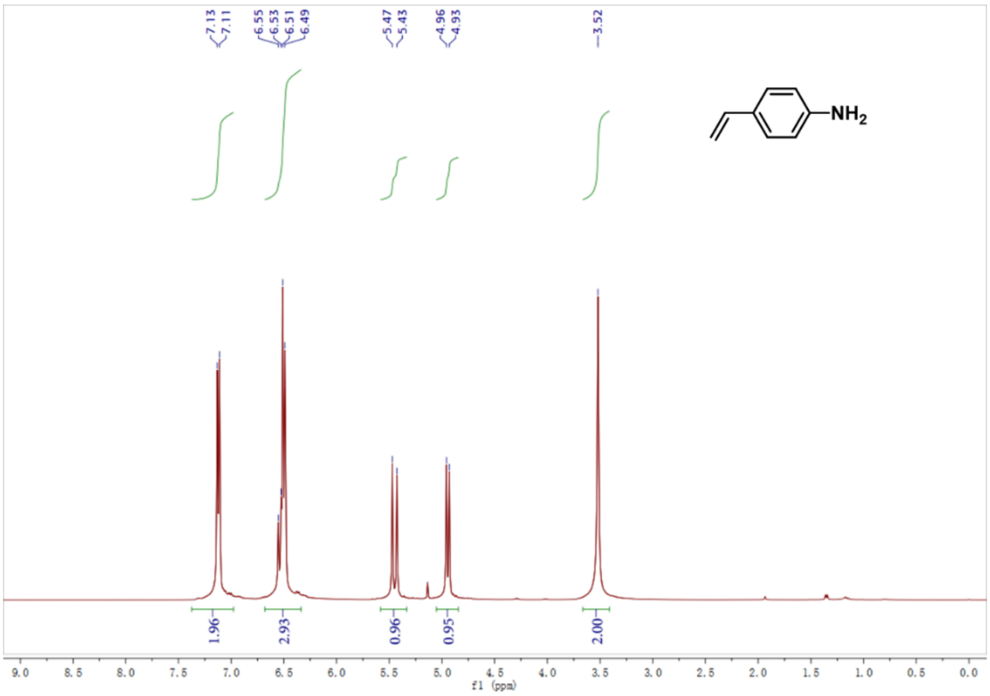

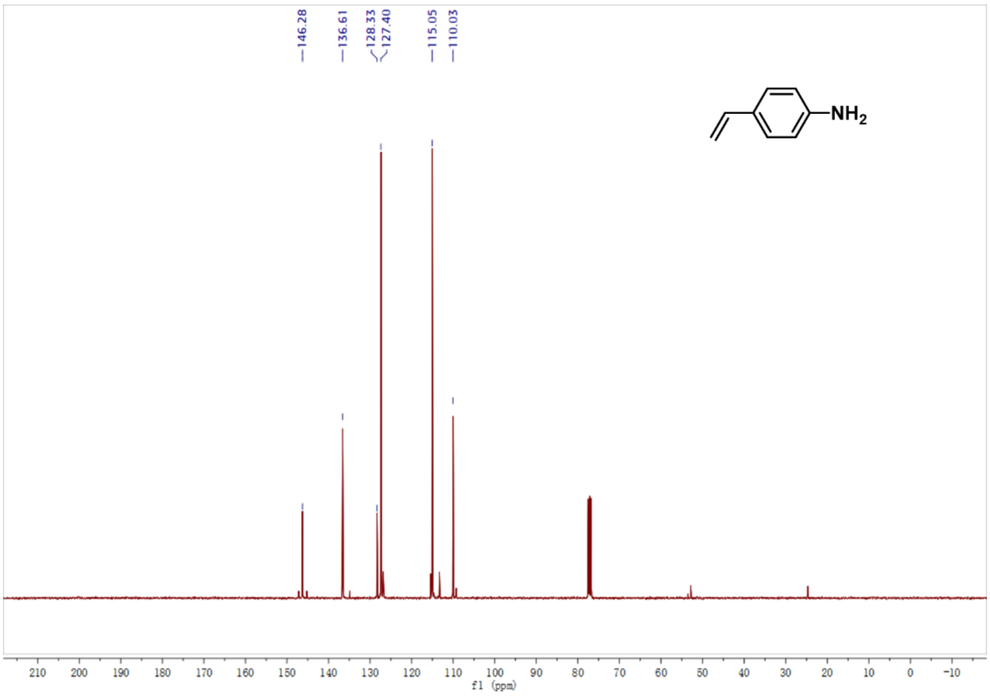

^{1}H and ^{13}C NMR Spectra of (*E*)-*N*-benzyl-1-phenylmethanimine (**4a**)

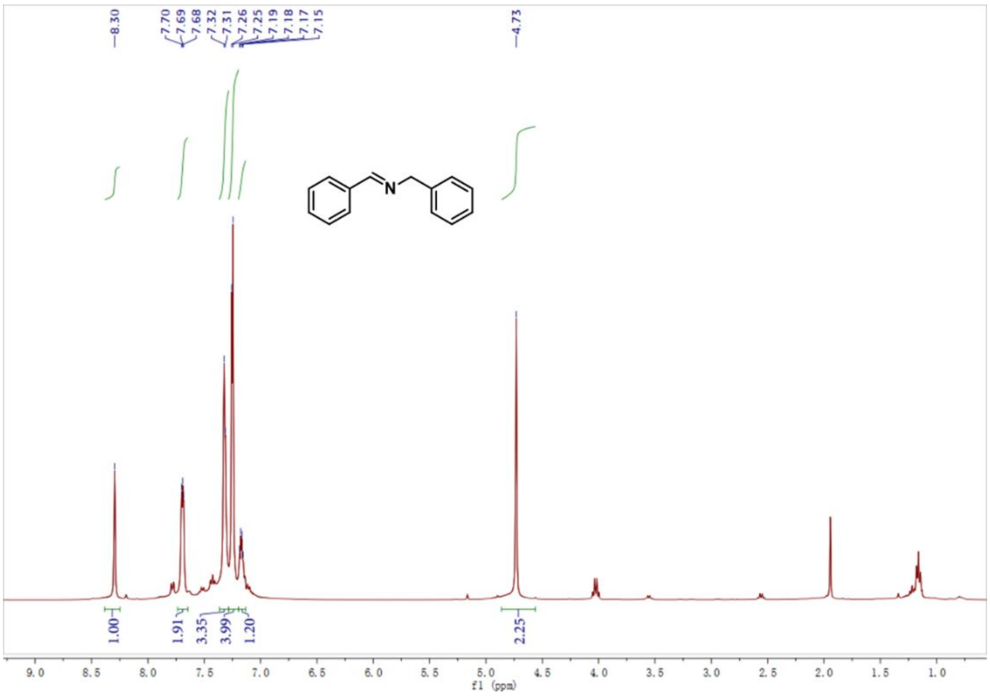

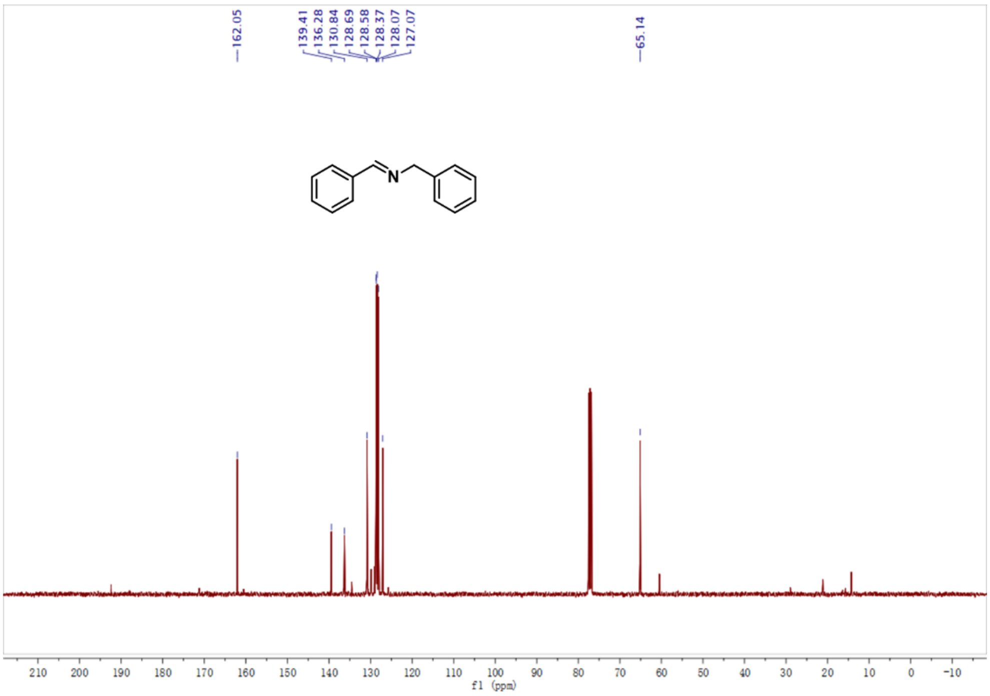

^{1}H and ^{13}C NMR Spectra of (*E*)-*N*-(4-methylbenzyl)-1-(p-tolyl)methanimine (**4b**)

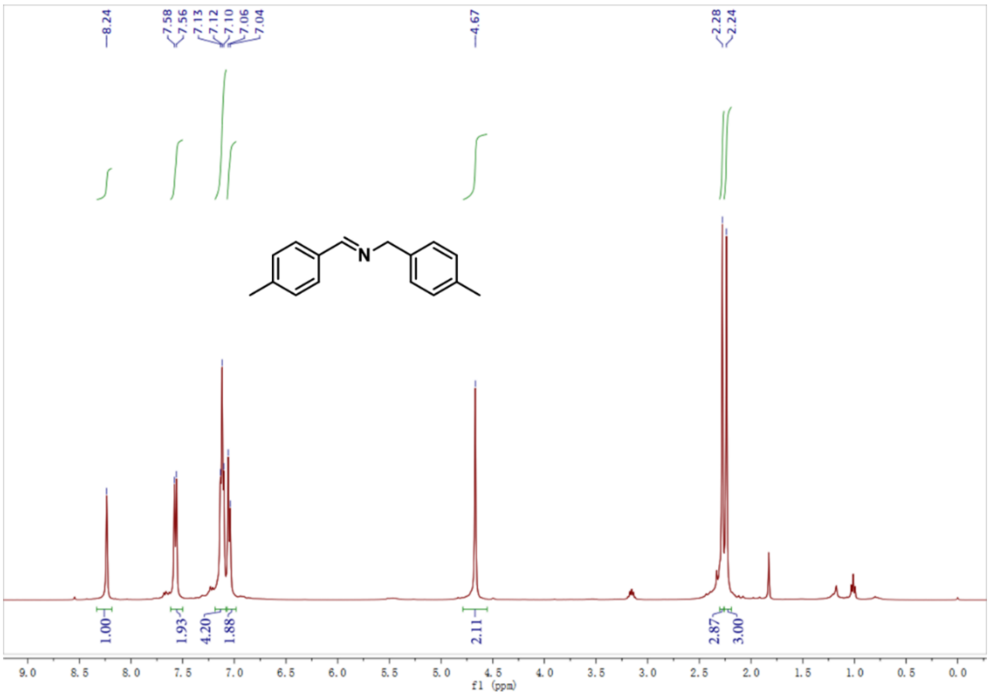

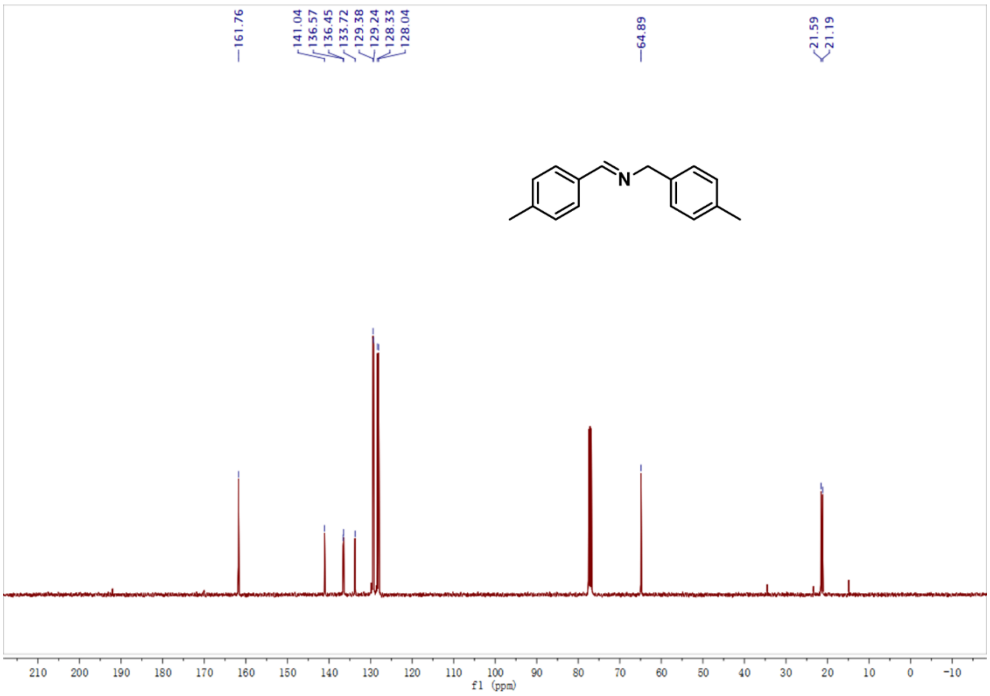

^{1}H and ^{13}C NMR Spectra of methyl (*E*)-4-(((4-(methoxycarbonyl)benzyl)imino)methyl)benzoate (**4c**)

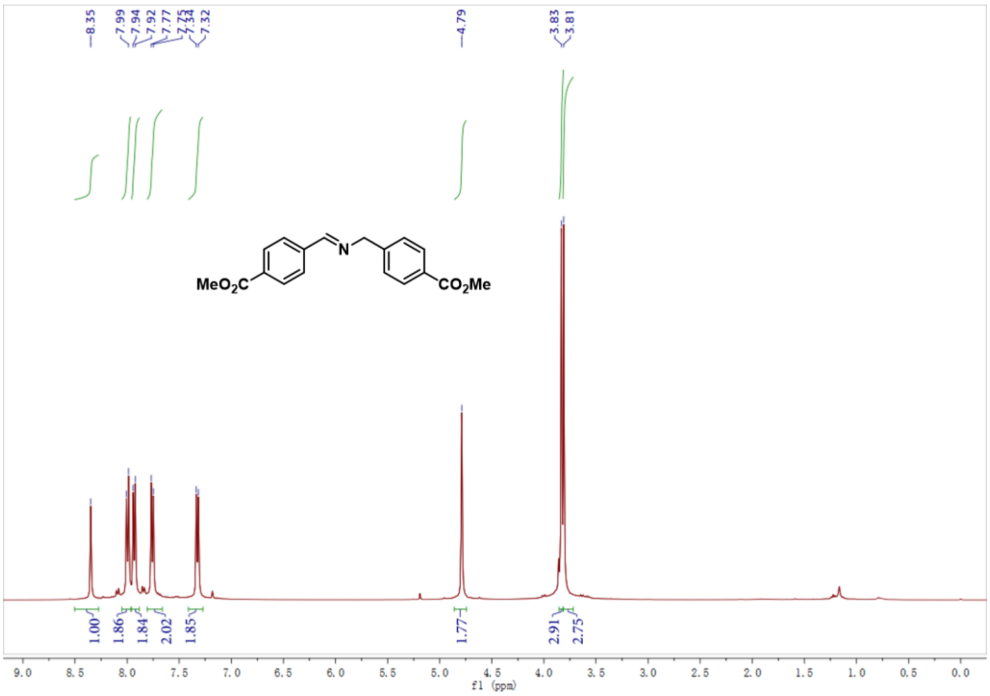

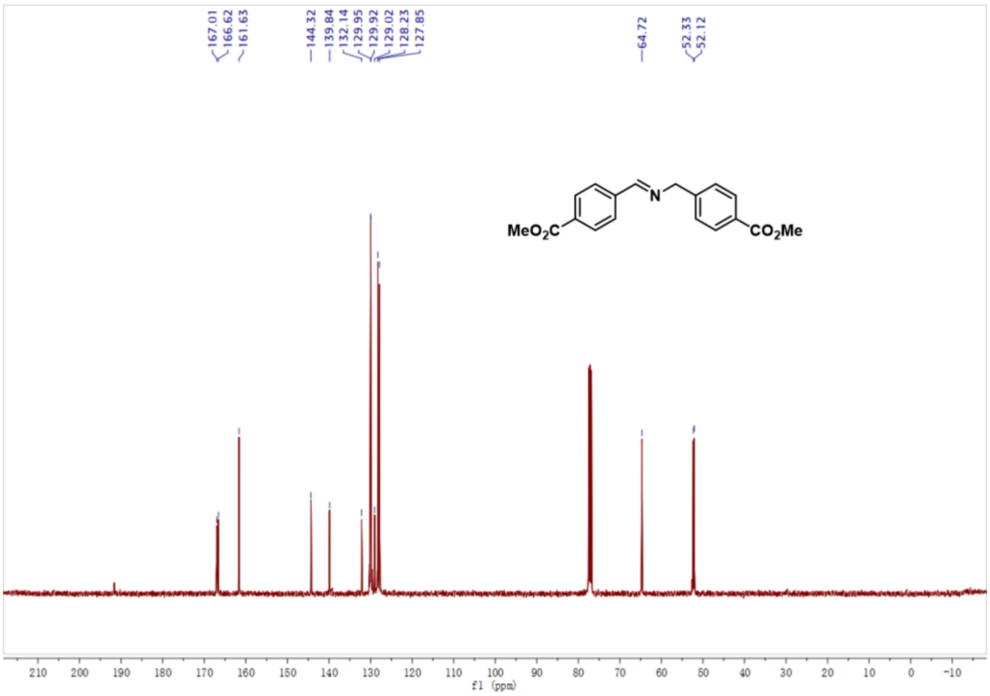

^{1}H and ^{13}C NMR Spectra of (*E*)-*N*-(4-(*tert*-butyl)benzyl)-1-(4-(*tert*-butyl)phenyl)methanimine (**4d**)

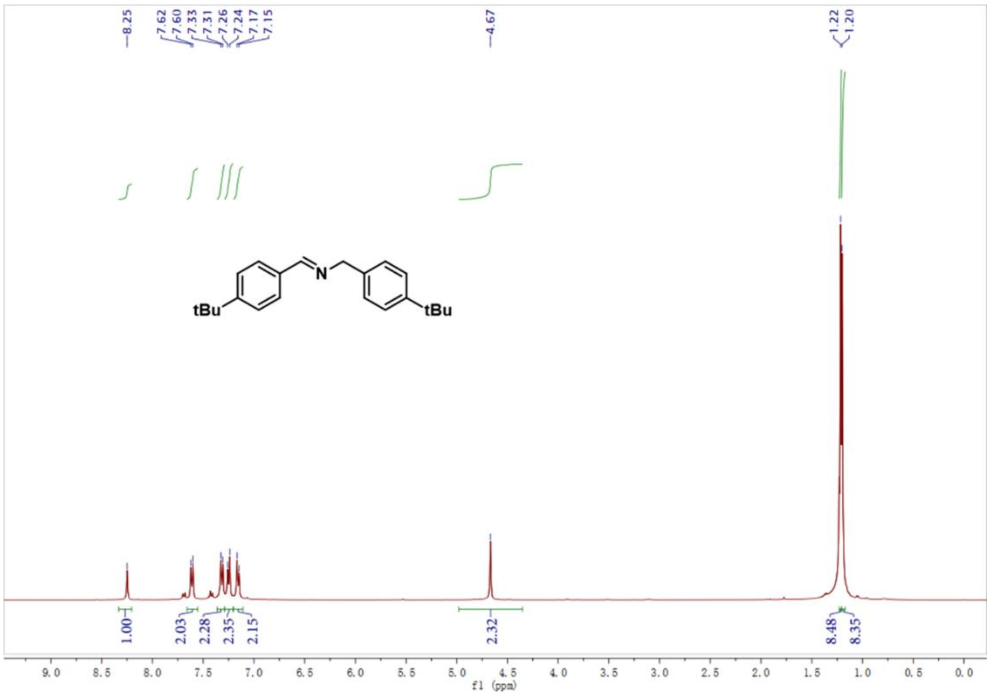

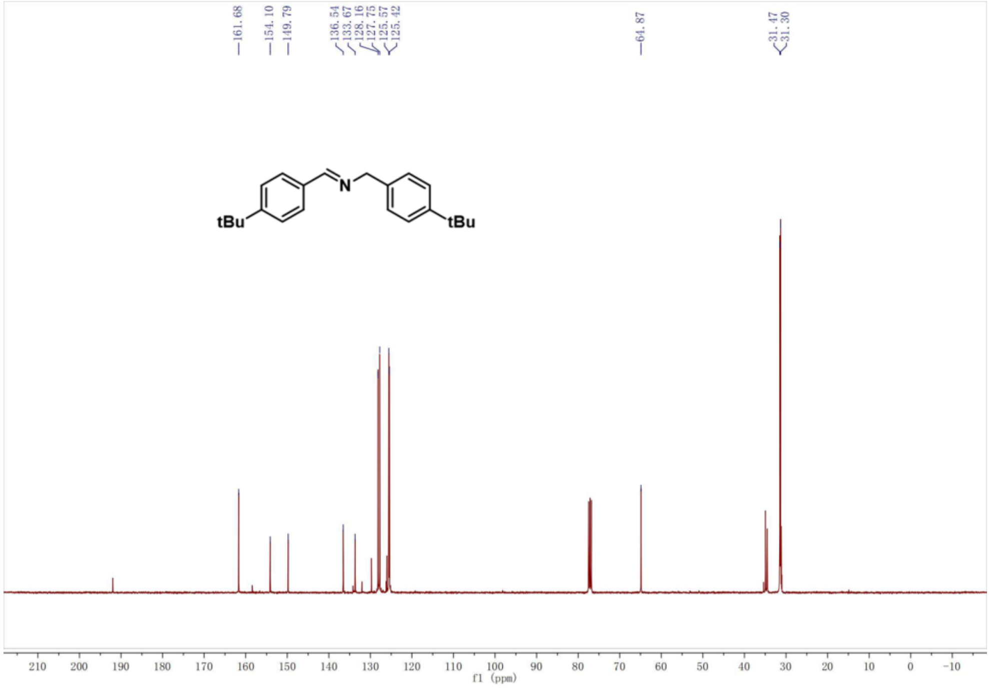

^{1}H and ^{13}C NMR Spectra of (*E*)-*N*-(4-chlorobenzyl)-1-(4-chlorophenyl)methanimine (**4e**)

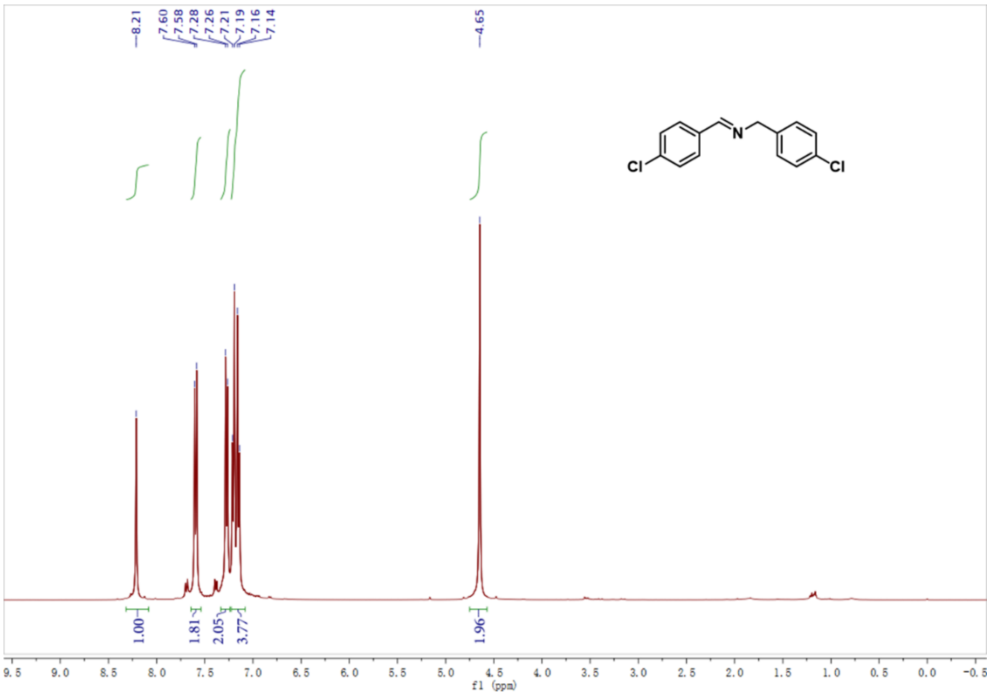

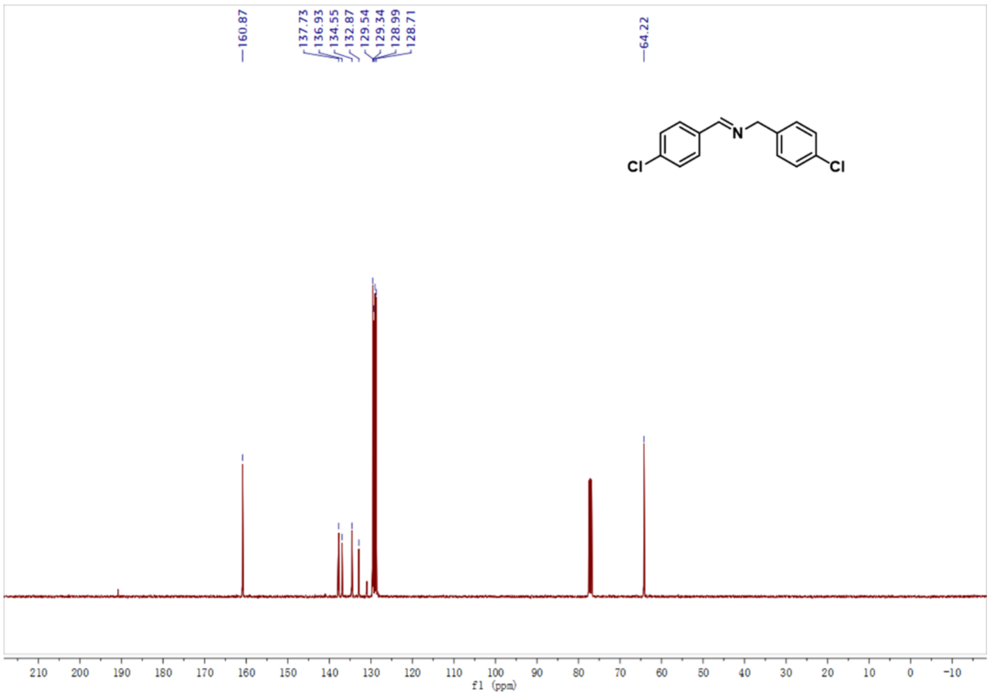

^{1}H and ^{13}C NMR Spectra of (*E*)-*N*-(4-bromobenzyl)-1-(4-bromophenyl)methanimine (**4f**)

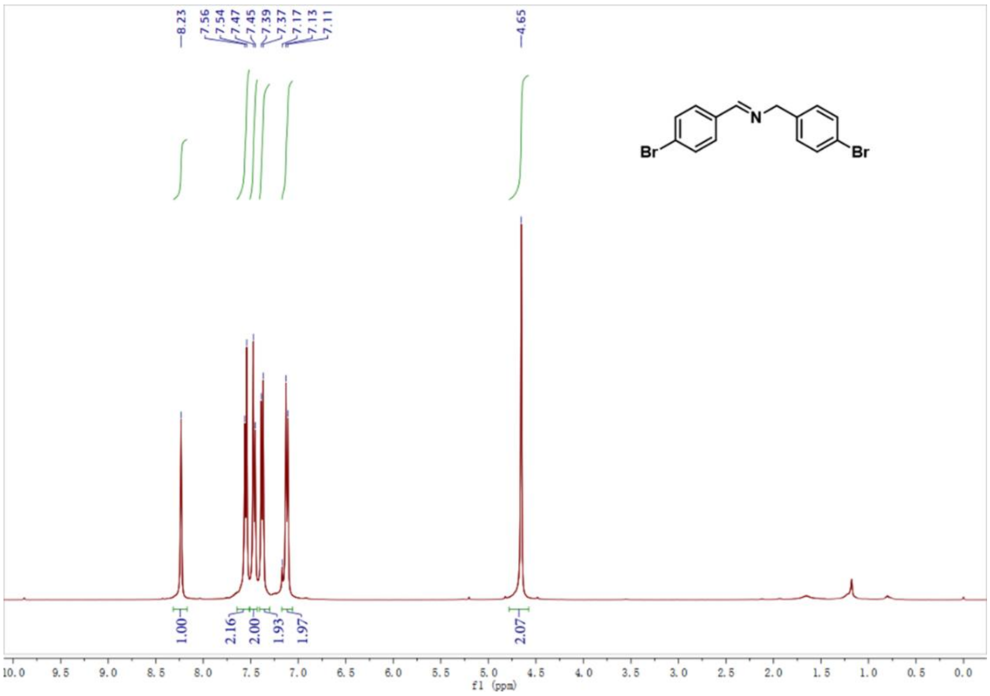

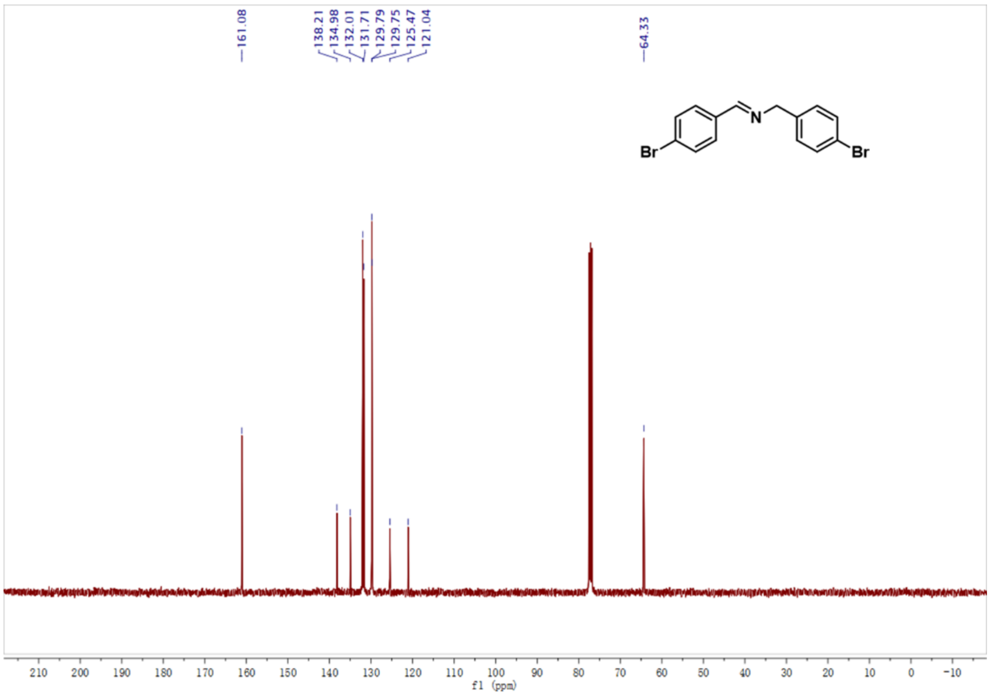

8. References

1. M. Rajesh, F. Dolhem, C. Davoisne and M. Becuwe, Reversible Anion Insertion in Molecular Phenothiazine-Based Redox-Active Positive Material for Organic Ion Batteries, *ChemSusChem*, 2020, **13**, 2364-2370.
2. D. Feng, Z. Y. Gu, J. R. Li, H. L. Jiang, Z. Wei and H. C. Zhou, Zirconium-Metalloporphyrin PCN-222: Mesoporous Metal–Organic Frameworks with Ultrahigh Stability as Biomimetic Catalysts, *Angew. Chem. Int. Ed.*, 2012, **51**, 10307-10310.
3. Z. Li, N. M. Schweitzer, A. B. League, V. Bernales, A. W. Peters, A. B. Getsoian, T. C. Wang, J. T. Miller, A. Vjunov, J. L. Fulton, J. A. Lercher, C. J. Cramer, L. Gagliardi, J. T. Hupp and O. K. Farha, Sintering-Resistant Single-Site Nickel Catalyst Supported by Metal–Organic Framework, *J. Am. Chem. Soc.*, 2016, **138**, 1977-1982.
4. B. Delley, An All-Electron Numerical Method for Solving the Local Density Functional for Polyatomic Molecules, *J. Chem. Phys.*, 1990, **92**, 508-517.
5. J. Sun, J. H. Liu, H. F. Su, S. M. Li, X. K. Tang, Z. L. Xie, Z. Xu, W. Y. Jiang, J. Y. Wei, X. K. Gong, A. He, S. Wang, D. E. Jiang, N. F. Zheng and H. Shen, Eight-Electron Copper-Hydride Nanoclusters: Synthesis, Structure, Alloying Chemistry and Photoluminescence, *Chem. Sci.*, 2025, DOI: 10.1039/d4sc08547g.
6. J. P. Perdew, K. Burke and M. Ernzerhof, Generalized Gradient Approximation Made Simple, *Phys. Rev. Lett.*, 1996, **77**, 3865-3868.
7. B. Delley, Hardness Conserving Semilocal Pseudopotentials, *Physical Review B*, 2002, **66**.
8. J. Jiao, H. Sun, C. Si, J. Xu, T. Zhang and Q. Han, Photocatalytic Multielectron Reduction of Nitroarenes to Anilines by Utilizing an Electron-Storable Polyoxometalate-Based Metal–Organic Framework, *ACS Appl. Mater. Interfaces*, 2022, **14**, 16386-16393.
9. M. f. Lv, G. p. Lu and C. Cai, Catalyst-Free Chemoselective Reduction of Nitroarenes Using Thiourea as a Hydrogen Source, *Asian J. Org. Chem.*, 2015, **4**, 141-144.
10. Y. Su, X. Li, Y. Wang, H. Zhong and R. Wang, Gold Nanoparticles Supported by Imidazolium-Based Porous Organic Polymers for Nitroarene Reduction, *Dalton Trans.*, 2016, **45**, 16896-16903.
11. K. Hyodo, G. Hasegawa, H. Maki and K. Uchida, Deacetylative Amination of Acetyl Arenes and Alkanes with C–C Bond Cleavage, *Org. Lett.*, 2019, **21**, 2818-2822.
12. W. Tang, Y. Liu, Y. Jin, Y. Wang, W. Shi, P. Ma, J. Niu and J. Wang, Photocatalytic Reduction of Nitrobenzene to Aniline by an Intriguing {Ru(C_6H_6)}-Based Heteropolytungstate, *Inorg. Chem.*, 2024, **63**, 6260-6267.
13. R. J. Lundgren, B. D. Peters, P. G. Alsabeh and M. Stradiotto, A P,N-Ligand for Palladium-Catalyzed Ammonia Arylation: Coupling of Deactivated Aryl Chlorides, Chemoselective Arylations, and Room Temperature Reactions, *Angew. Chem. Int. Ed.*, 2010, **49**, 4071-4074.
14. S. Hazra, A. K. Kushawaha, D. Yadav, P. Dolui, M. Deb and A. J. Elias, Table Salt as a Catalyst for the Oxidation of Aromatic Alcohols and Amines to Acids and Imines in Aqueous Medium: Effectively Carrying Out Oxidation Reactions in Sea Water, *Green Chem.*, 2019, **21**, 1929-1934.
15. R. D. Patil and S. Adimurthy, Copper-Catalyzed Aerobic Oxidation of Amines to Imines under Neat Conditions with Low Catalyst Loading, *Adv. Synth. Catal.*, 2011, **353**, 1695-1700.
16. T. Bosanac and C. S. Wilcox, Precipiton Reagents: Precipiton Phosphines for Solution-Phase Reductions, *Org. Lett.*, 2004, **6**, 2321-2324.
17. M. Rueping, C. Vila, A. Szadkowska, R. M. Koenigs and J. Fronert, Photoredox Catalysis as an Efficient Tool for the Aerobic Oxidation of Amines and Alcohols: Bioinspired Demethylations and Condensations, *ACS Catalysis*, 2012, **2**, 2810-2815.